IMES DISCUSSION PAPER SERIES

Current Status and Future Prospects of Optical Quantum Computing

Toshikazu Hashimoto and Kazutoshi Kan

Discussion Paper No. 2026-E-10

IMES

INSTITUTE FOR MONETARY AND ECONOMIC STUDIES

BANK OF JAPAN

2-1-1 NIHONBASHI-HONGOKUCHO
CHUO-KU, TOKYO 103-8660
JAPAN

You can download this and other papers at the IMES Web site:

https://www.imes.boj.or.jp

Do not reprint or reproduce without permission.

NOTE: IMES Discussion Paper Series is circulated in order to stimulate discussion and comments. The views expressed in Discussion Paper Series are those of authors and do not necessarily reflect those of the Bank of Japan or the Institute for Monetary and Economic Studies.

IMES Discussion Paper Series 2026-E-10

August 2026

Current Status and Future Prospects of Optical Quantum Computing

Toshikazu Hashimoto* and Kazutoshi Kan**

Abstract

This paper introduces the principles and implementation of continuous-variable optical quantum computing (CV-OQC) and provides an overview of the current status and challenges of its research and development. The optical approach is considered a strong candidate for realizing large-scale, fault-tolerant quantum computers, as it enables large-scale quantum entanglements to be generated by using optical qubits that retain their quantum nature even at room temperature. Many of the CV-OQC technologies are adapted from existing optical communication technologies. However, numerous technical challenges remain, including the implementation of quantum error correction and cubic phase gate operations for achieving quantum advantage. These challenges span a broad range, from hardware problems to software issues, and they need to be addressed integrally within the control circuitry. Thus, the advancement of CV-OQC necessitates collaboration among research institutions and companies with diverse strengths. Moreover, despite the numerous hurdles, CV-OQC technologies for transmitting and manipulating optical quantum states would also be beneficial to other approaches to quantum computing and communication. Thus, continued research and development in this area would be highly valuable.

Keywords: Optical Quantum Computing; Measurement-Based Quantum Computing; Gottesman-Kitaev-Preskill Code

JEL classification: L86, L96, O36

* Senior Distinguished Researcher, NTT Device Technology Laboratories (E-mail: toshikazu.hashimoto@ntt.com)

** Director, Institute for Monetary and Economic Studies, Bank of Japan (currently Financial System and Bank Examination Department, E-mail: kazutoshi.kan@boj.or.jp)

This paper is contract research from the Institute for Monetary and Economic Studies, Bank of Japan. The authors would like to express their gratitude to Associate Professor Shuntaro Takeda (The University of Tokyo) and Professor Noboru Kunihiro (University of Tsukuba) for their valuable comments. The views expressed in this paper are solely those of the authors and do not represent the official views of the Bank of Japan. This paper was written on the basis of information available as of March 2025.

Table of Contents

I. Introduction

Quantum computing is a computational technology that leverages the principles of quantum mechanics. In general, all particles at microscopic scales exhibit quantum mechanical properties. To date, various approaches to quantum computing have been explored, including those based on optical systems, superconducting circuits, neutral atoms, and trapped ions. Each of these approaches is a prominent candidate for realizing a practical quantum computer (i.e., a large-scale fault tolerant quantum computer), but each also has its own strengths and weaknesses. It remains uncertain which of these approaches will ultimately lead to practical quantum computing. This paper focuses on one such approach, **continuous variable optical quantum computing** (CV-OQC), and outlines its current state of research and development, as well as its challenges.

Optical quantum computing (OQC) can be broadly categorized into two approaches: one that uses **photons**, whose energies are quantized[1], and another, i.e., CV-OQC, that utilizes **coherent light**[2] that encodes quantum information in the complex amplitude[3] of the electromagnetic field of coherent light, such as from laser beams. The former approach requires precise control over individual photons, making it technically demanding. In contrast, the latter approach is considered a more promising one for realizing practical quantum computing systems.

In particular, CV-OQC offers three major advantages. First, optical quantum states remain stable at room temperature. More precisely, they are not susceptible to thermal noise or disturbances from the environment. As a result, CV-OQC does not require costly cooling systems or large-scale apparatus. In comparison, superconducting quantum computers must be kept at extremely low temperatures by enclosing the entire system in a refrigeration unit to eliminate thermal noise. Similarly, approaches using neutral atoms or ions rely on trapping these particles in space by using laser light or electromagnetic fields respectively

---

[1] In the field of physics, the term "quantum" refers to the concept of discreteness in mathematics. The energy of extremely weak light cannot take continuous values but instead exhibits discrete levels. In physics, such natural laws are conventionally described as being "quantized." A continuous-variable quantum system refers to a special type of physical system whose states are represented by continuous values while still exhibiting quantum mechanical properties.

[2] Coherent light refers to light composed of a large number of photons sharing a common phase. For further details, see Section 2.

[3] A complex amplitude is a complex number that simultaneously represents the phase and amplitude of a quantum wave. Once its real and imaginary components are specified, both the phase and amplitude are uniquely determined.

to isolate them from environmental noise, which necessitates large and complex equipment.

Second, CV-OQC allows for the generation, maintenance, and manipulation of large-scale quantum entanglements, which are essential for large-scale quantum computing, in a relatively straightforward manner.

Third, since CV-OQC manipulates quantum states as optical pulses,[4] it is believed that by leveraging high-speed optical communication technologies, information processing speeds equivalent to clock frequencies in the terahertz (THz) range, i.e., processing of up to 10^{12} pulses per second, can be achieved.

Nevertheless, CV-OQC has several drawbacks. First, it is known to be difficult to implement nonlinear operations required for universal quantum computing using currently available optical materials. Second, since light always propagates at the speed of light and possesses extremely high frequencies, even slight differences in optical paths can alter interference conditions, potentially introducing significant computational errors. Thus, it is extremely challenging to align and synchronize multiple optical paths spatially for computing while ensuring stable interactions. Third, although optical quantum states are robust to thermal noise, they are affected by optical loss, corresponding to the disappearance of photons. This optical loss is a challenge unique to optical systems and is not typically encountered in platforms using neutral atoms or ions. In the CV-OQC approach, minimizing optical loss is crucial at every stage, i.e., in the generation, maintenance, and manipulation of quantum states.

To address the first and second drawbacks, a computational model known as **measurement-based quantum computing** (MBQC) has been proposed. MBQC has opened up new possibilities for CV-OQC, which previously struggled to implement strong nonlinear operations. However, even within the MBQC framework, the third challenge—loss suppression—remains a major challenge.

While many of the technologies required for CV-OQC can be supported by existing optical components and optical fiber communication technologies, several unresolved challenges remain. The most notable of these pertain to **quantum error correction**, which is necessary to mitigate the effects of noise during computation. Addressing them will require both theoretical and practical advancements.

In the context of finance, while quantum computing raises concerns about

[4] An optical pulse refers to a wave of light that is emitted for a short period of time. In optical communication technologies, such pulses are used to carry information signals.

threats such as cryptographic decryption, it also offers potential benefits, including faster pricing of securitized products and reductions in computational energy consumption. For example, it could lead to decreased electricity demand for Bitcoin mining. Furthermore, OQC, with its high operating frequency (clock rate), may contribute to cost savings and environmental impact reductions even without achieving **quantum advantage**, [5] by enabling fast and energy-efficient computations. Therefore, although the realization of a practical quantum computer remains a distant goal, it is nonetheless beneficial for the financial industry to understand both the risks and the potential of CV-OQC.

The remainder of this paper is structured as follows: Section II explains the quantum states used in the CV-OQC. Section III describes the principles of MBQC. Section IV introduces the optical device technologies for hardware implementations. Section V identifies the technical challenges. Section VI concludes the paper.

Sections II through IV focus primarily on technical content. Readers who are mainly interested in the current status, challenges, and significance of research on the CV-OQC are encouraged to refer to Sections V and VI. A List of Symbols used in this paper is provided prior to the Appendices.

II. CV Optical Quantum States and Their Manipulation

In this section, we explain the quantum states that serve as the fundamental units of information in quantum computing. Most quantum computing approaches like those based on neutral atoms or ions manipulate various physical quantum mechanical systems that have discrete energy levels and that can be directly treated as **quantum bits** (or **qubits**), i.e., superpositions of 0 and 1. In contrast, CV-OQC employs continuous physical states from quantum optics such as the **coherent state** and the **squeezed state**. These states are characterized by the (complex) amplitude of light that exhibits quantum mechanical properties and are collectively referred to as **continuous-variable optical quantum states**.

The Section II.B begins with an explanation of coherent states, which are general continuous-variable quantum states not limited to optical systems. It then describes **coherent light**, which is the optical version of the coherent state; **orthogonal squeezed light**, which corresponds to the qubit basis of other quantum computing approaches; and **time-domain multiplexing**, which

[5] **Quantum advantage** or **quantum supremacy** refers to a phenomenon that a quantum computer solves certain problems efficiently, which classical computers cannot solve efficiently.

allocates squeezed light pulses to distinct time intervals (time slots). Figure 1 illustrates the preparation of these quantum states.

Figure 1 Preparation of Continuous-Variable Optical Quantum States

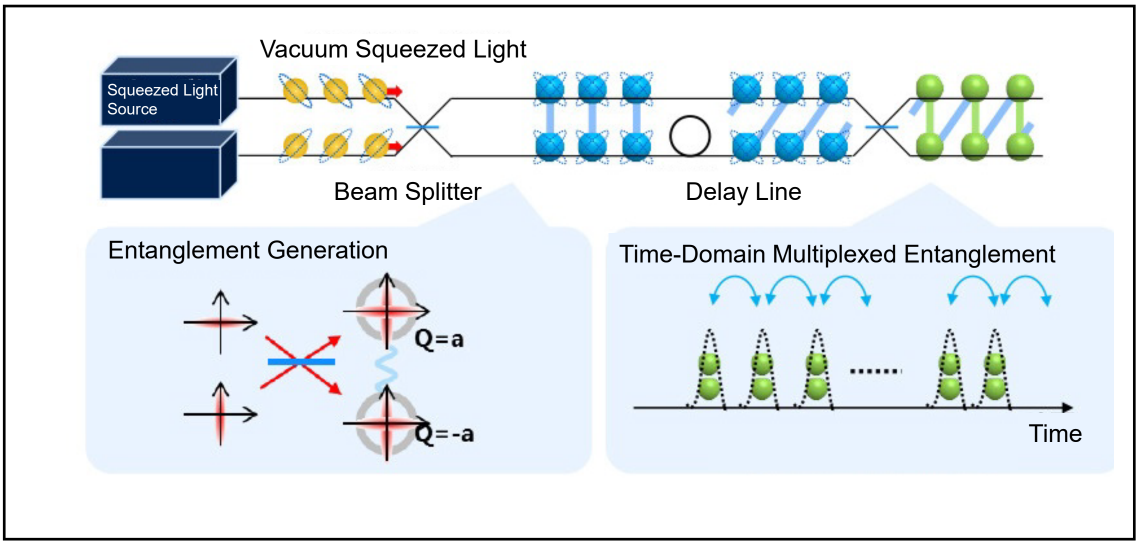

A. Advantages of CV Quantum States

As mentioned above, most quantum computing schemes represent quantum information as **superpositions** of two discrete states, "0" and "1." They operate on these **qubits** by applying physical operations that correspond to mathematical operations. Qubits are typically **entangled**, meaning their states are interdependent. Since these schemes encode quantum information into discrete values, we will refer to this approach as **discrete-variable (DV) quantum computing**.

In contrast, the quantum information used in CV-OQC is characterized by continuous variables. In many cases, the information is embedded in a macroscopic many-particle system that exhibits quantum mechanical properties, specifically known as coherent states, as discussed later. Although the coherent states do not take on only discrete values, they exhibit phenomena such as superposition and entanglement, making them for useful for quantum information processing.

CV-OQC offers several advantages over DV quantum computing. First, operations on coherent states are classical, so they are inherently more robust to noise and easier to implement. In contrast, DV quantum information processing tasks typically require delicate and noise-sensitive control. Second, because a single CV quantum state consists of a large number of particles (photons), its multiple degrees of freedom can be exploited to perform tasks such as **quantum error correction** easily. By contrast, quantum error correction using DV quantum states tends to be more complex—for example, requiring coordinated operations (transport) on an entire group of physical qubits when a single logical qubit has to be moved to another part of the processing device.

B. Coherent States

The Section II.B elaborates on the first of the advantages described above, namely, the ability to manipulate quantum states using classical operations. A typical example of such a manipulable state is the coherent state.

A **coherent state** can be regarded as an approximate classical state of a many-particle system where all particles occupy the same quantum state. A typical example is laser light, which is composed of many photons all having almost the same frequency and a synchronized phase relationship. In the context of hardware development for CV-OQC, coherent states are often referred to simply as **laser light**; in more theoretical discussions, they are referred to as **coherent light**. In this paper, both terms will be used interchangeably. For further details on coherent light, see Appendix 1.C.

A coherent state of a specific mode (defined by its frequency and the direction of oscillation) can be regarded as a classical-like wave and fully characterized by two parameters: **amplitude**, which represents the strength of oscillation; and **phase**, which indicates the position within the oscillation cycle. These two parameters constitute the **complex amplitude**, which can equivalently be decomposed into the **cosine and sine components** of the oscillation. For mathematical convenience, these components are represented as the real and imaginary parts of the complex amplitude.

According to the **uncertainty principle**, the product of the spreads (variances) in the cosine and sine components has a lower bound. A coherent state is defined as a quantum state that achieves this minimum bound, thus closely approximating a classical state. Coherent states exhibit the following properties:

- A coherent state is specified by continuous parameters in **phase space**. For example, in classical mechanics, the motion of a body can be represented as a trajectory in a phase space composed of position and momentum coordinates. More generally, we can think of phase space as a way of representing the evolution of physical states.

- Although a coherent state is a superposition of many particle states, each particle maintains **coherence**—that is, a consistent phase—with respect to its location in phase space. As a result, the many-particle system forms a unified state.
- Because a coherent state is a superposition of coherently phased particle states, its evolution also preserves coherence. This makes the coherent state stable and resistant to decoherence. Furthermore, its temporal evolution closely resembles classical trajectories in phase space.
- A coherent state possesses symmetries, so that it remains invariant under certain operations. Thus, it is less susceptible to disturbances from those operations.

These properties are naturally realized in CV-OQC through the use of laser light, and for that reason, they are not always emphasized in discussion. However, they are crucial for CV-OQC. This paper will not describe any further on the properties of coherent states; interested readers may consult Dey, Samuel, and Vidyarthi [2022] and Kuratsuji [2005].

C. Coherent Light and Squeezed Light

The state of **coherent light** is uniquely specified by its complex amplitude. Each component of the complex amplitude takes on continuous values. Thus, the phase space of coherent light is a two-dimensional plane whose axes are the **cosine and sine components**, or equivalently, the **real and imaginary parts of a complex amplitude**. In this phase space, coherent light appears as a quantum state whose quantum fluctuations (i.e., probability distribution of presence) spread isotropically around a central point (see Figure 2(a)).

Figure 2 Coherent Light and Squeezed Light

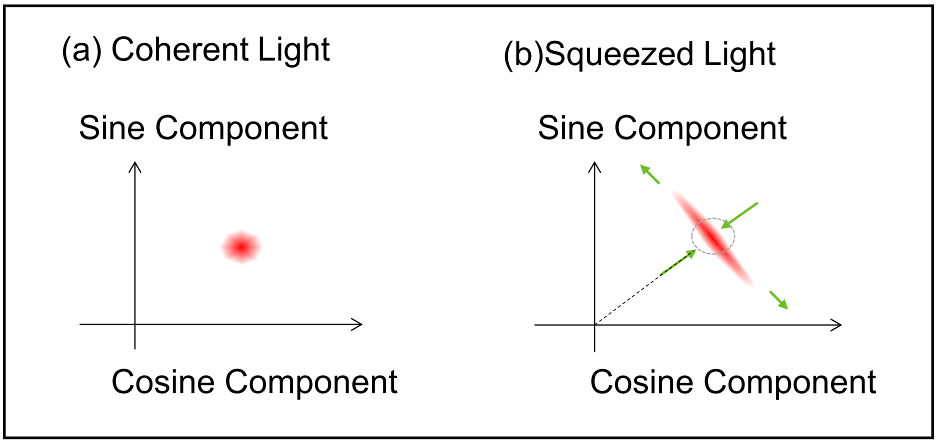

In contrast, **squeezed light** refers to a state in which the quantum fluctuations of coherent light are narrowed along one axis in phase space and broadened along the orthogonal axis (see Figure 2(b)). Visually, this corresponds to a deformation of the quantum state in phase space—stretching it in one direction and "squeezing" it in the other.

Note that due to the uncertainty principle, the spread of quantum fluctuations in phase space cannot be reduced below a certain limit. For the mathematical treatment of squeezed light, refer to Appendix 1.D and 1.E.

CV-OQC uses two squeezed light states that are stretched approximately orthogonal to one another and can thus be distinguished by making **quadrature phase amplitude measurements** (hereafter **quadrature measurements**, see Section IV for details). As such, they can serve as distinguishable logical states analogous to "0" and "1" in qubit-based systems. Furthermore, these states can be passed through a half mirror to generate quantum entanglements, which can then be utilized in computations. Here, the half mirror functions as an optical element—a beam splitter—that divides incoming light into two or more paths. For the mathematical background, see Appendix 4.

D. Time-Domain Multiplexing

In the CV-OQC approach, it is possible to increase the dimensionality of distinguishable states not only through varying the orientation of the squeezing , but also by varying the delay of the optical pulses. This technique is called **time-domain multiplexing**.

Time-domain multiplexing assigns each pulse to a distinct time slot (i.e., **time bin**) and treats it as a distinguishable quantum state. Physically, this is achieved by operations that delay the propagation of optical pulses along the optical path by N pulse intervals. This method of representing quantum states is referred to as **time-bin encoding**.

It is also possible to generate superposition and quantum entanglement between quantum states in different time slots.

E. Comparison Between DV and CV Quantum Computing

Which approach, DV or CV quantum computing, is superior in general? In this section, we offer some preliminary considerations from the perspective of computational errors induced by environmental noise or computational operations.

In **classical computing** (i.e., conventional computation without qubits), the fundamental difference between discrete and continuous data lies in the ease of error correction. In the case of discrete data (digital data), errors caused by noise can be corrected easily and accurately through digital processing, as long as they remain below a certain threshold. By contrast, in the case of continuous data (analog signals), it is often difficult to distinguish between corrupted and valid data, making error correction inherently challenging. However, continuous signals can be digitized [6] through sampling. Although digitization itself introduces some error, according to the **sampling theorem**, a continuous signal can be perfectly reconstructed if it is sampled at a rate greater than twice its highest frequency component.

In the modern era, the computational cost of signal reconstruction has been dramatically reduced thanks to large-scale integration (LSI) technologies. Thus, when the frequency bandwidth of the target signal is limited, the prevailing trend is to digitize continuous signals and leverage the robustness of digital error correction.

Error correction is also essential in quantum computing. Moreover, its difficulty differs between DV and CV quantum computing. In the DV case, the error rate is non-negligible, which necessitates encoding logical information across many **physical qubits**. A virtual qubit composed of many physical qubits through error correction serves as a noise-robust digital unit: a **logical qubit**. Moreover, since the measurement can alter the quantum state, one must correct

[6] For example, since the audible frequency range is roughly below 20 kHz, the sampling rate for compact discs is set at 44.1 kHz. Based on such results from the sampling theorem, many analog devices have been replaced by digital counterparts.

errors without directly measuring the physical qubits one wishes to verify. This fact further increases the number of physical qubits required for fault-tolerant encoding. Several error-correcting codes for physical qubits have been proposed, such as **stabilizer codes** and **surface codes**, and experimental studies have accumulated accordingly.

Conversely, in CV systems, it is preferable to avoid representing quantum states via physical qubits or traditional analog-to-digital approximations. Instead, an effective error correction scheme must leverage the continuous nature of the state. **GKP code** proposed by Gottesman, Kitaev, and Preskill [2001], for instance, discretizes the CV phase space at regular intervals, encoding information in a superposition of those discrete points. By suppressing analog errors, the encoded state functions as a logical qubit.

Regarding error correction of DV and CV quantum states, future technological developments will no doubt determine which approach is ultimately superior. At present, there is a gradual but noticeable synergy between research efforts in error correction for both systems. In DV quantum error correction, techniques incorporating multi-level encoding, which are conceptually analogous to multivalued logic in classical systems, have been proposed, such as **bosonic codes**,[7] which are closely related to GKP code. Conversely, in CV quantum error correction, due to implementation constraints and other factors, it is difficult to achieve sufficient error-correcting performance with imperfect GKP encodings. To address this issue, approaches inspired by DV quantum error correction techniques have been proposed, in which such imperfect GKP qubits are combined or concatenated with qubit codes to construct more robust logical qubits. Thus, rather than prematurely declaring one technology categorically superior, it should be realized that there is significant value in continuing to pursue research and development on both DV and CV quantum error correction.

[7] A bosonic code is a general term for quantum error-correcting codes based on CV quantum systems. The term "bosonic" is used because a realization of a CV quantum system requires bosons such as photons.

III. CV Quantum Computation

A promising computational model for CV-OQC is **measurement-based quantum computing (MBQC)**, which leverages CV-OQC's advantage that large-scale quantum entangled states can be generated relatively easily. In MBQC, a large-scale entangled state is prepared before the computation, which then proceeds by sequentially performing measurements on parts of that state. Moreover, GKP code is considered a promising candidate for quantum error correction in this model. Since these techniques differ significantly from those used in other major approaches to DV quantum computing, which typically rely on performing quantum gate operations on qubits, this section is structured as follows: Section III.A introduces the paradigm of quantum gate operations in CV systems, in contrast to the DV systems. Section III.B explains MBQC. Section III.C discusses the GKP code.

A. Quantum Gate Operations in CV Systems

In DV quantum computing, computation is carried out by applying a sequence of **quantum gate operations** to qubits. In CV quantum computing, similar gate operations are performed on CV quantum states. This subsection introduces quantum gate operations for CV systems by comparing them with those of DV systems. Table 1 summarizes the main gate operations for qubits and CV quantum states.

Table 1 Gate Operations for Qubits and CV Quantum States

	Qubit		CV Quantum State	
Clifford Gates **Gaussian Gates** (**Efficiently Computable on Classical Computers**)	Bit−Flip Gate $\hat{\sigma}_x$	Computational Basis $\{\|0\rangle, \|1\rangle\}$	x Displacement Gate $\hat{X}(s) = e^{-2is\hat{p}}$	Computational Basis $\{\|x\rangle \mid x$ is position$\}$
	Phase−Flip Gate $\hat{\sigma}_z$	Conjugate Basis $\{\|+\rangle, \|-\rangle\}$	p Displacement Gate $\hat{Z}(s) = e^{2is\hat{x}}$	Conjugate Basis $\{\|p\rangle \mid p$ is momentum$\}$
	Controlled−NOT Gate $\|x\rangle\|x'\rangle \to \|x\rangle\|x + x' \bmod 2\rangle$		Quantum Non−Demolition Gate $\|x\rangle\|x'\rangle \to \|x\rangle\|x + x'\rangle$	
Non-Clifford Gate **Non-Gaussian Gate** (**Non-Classicality-Inducing**)	T Gate $\hat{T} = \begin{pmatrix} 1 & 0 \\ 0 & e^{i\pi/4} \end{pmatrix}$		Cubic Phase Gate $\exp(i\gamma\hat{x}^3)$	

1. Gate Operations in DV Quantum Systems

A qubit is a quantum state constructed from two distinguishable basis states, typically labeled "0" and "1." These states are often abstracted using the notion of **spin**,[8] which represents the fundamental unit of a magnetic moment. A spin does not have degrees of freedom associated with its magnitude as a vector, but it does have freedom in its spatial orientation along the x-, y-, and z-axes. When measuring the spin along a particular direction—say, the z-axis—the result is either aligned with the positive direction or the negative direction of that axis. These two outcomes are referred to as **spin-up** and **spin-down** and are commonly mapped to the logical states $|0\rangle$ and $|1\rangle$ of a qubit.

The computational basis states, spin-up and spin-down, are represented as the following column vectors:

$$|0\rangle = \begin{pmatrix}1\\0\end{pmatrix}, |1\rangle = \begin{pmatrix}0\\1\end{pmatrix}.$$

A general qubit state is expressed as a linear combination of these basis states:

$$\alpha|0\rangle + \beta|1\rangle$$

where α and β are complex coefficients. The squares of the absolute values of these coefficients, $|\alpha|^2$and$|\beta|^2$, represent the probabilities of measuring the qubit in the $|0\rangle$ and $|1\rangle$ states, respectively. Thus, the sum of those values must satisfy the normalization condition $|\alpha|^2 + |\beta|^2 = 1$. Operations corresponding to specific transformations of the spin along the x-, y-, and z-axes can be represented (up to a scalar normalization with respect to the z-basis) by the following matrices:

$$\hat{\sigma}_z = \begin{pmatrix}1 & 0\\0 & -1\end{pmatrix}, \hat{\sigma}_x = \begin{pmatrix}0 & 1\\1 & 0\end{pmatrix}, \hat{\sigma}_y = \begin{pmatrix}0 & -i\\i & 0\end{pmatrix}.$$

Among these, $\hat{\sigma}_x$ and $\hat{\sigma}_y$ correspond to operations that flip or rotate the spin, i.e., they change the direction of the spin. $\hat{\sigma}_z$ corresponds to applying a magnetic field along the z-axis, while $\hat{\sigma}_x$ and $\hat{\sigma}_y$ correspond to applying transverse magnetic fields along the x- and y-axes, respectively.[9, 10] These matrices are collectively known as the **Pauli matrices**.

[8] Spin is an intrinsic quantum-mechanical angular momentum associated with a magnetic moment; measurement along one direction makes other components indeterminate, unlike in the classical case.

[9] Operations corresponding to those are physically implementable in superconducting current-based qubits. In such case, those operations are performed with resonant microwave pulses.

[10] The operator $\hat{\sigma}_z$ has eigenvalues 1 and -1, corresponding to spin-up and spin-down states, respectively.

Among these, the x-axis operation $\hat{\sigma}_x$ is, as is evident from its matrix form, a **bit-flip gate** that swaps the states $|0\rangle$ and $|1\rangle$. Next, consider the superposition states,

$$|\pm\rangle = \frac{1}{\sqrt{2}}(|0\rangle \pm |1\rangle).$$

In this basis, the operator $\hat{\sigma}_z$ acts as a **phase-flip gate**: it inverts the phase of the $|1\rangle$ component relative to $|0\rangle$.

Another important operation is the **controlled-NOT (CNOT) gate**, which operates on two qubits: a **control bit** in state $|x\rangle$ and a **target bit** in state $|x'\rangle$. The operation is defined as:

$$\hat{U}_{\text{CNOT}}|x\rangle|x'\rangle = |x\rangle|x' + x \bmod 2\rangle.$$

That is, it flips the target bit if the control bit is in the state $|1\rangle$, and does nothing if the control bit is $|0\rangle$.

These three fundamental gates are called as the **Clifford gates**. It is known (via the **Gottesman–Knill theorem**) that any quantum computation composed solely of Clifford gates can be efficiently simulated on a classical computer. Therefore, quantum computation limited to Clifford gates cannot achieve a quantum advantage in the sense of computational complexity.

To achieve a quantum advantage, **non-Clifford gates** are required. A commonly used non-Clifford gate is the $\boldsymbol{\pi/4}$ **gate**, also called the **T gate**, which is represented by the matrix,

$$\hat{T} = \begin{pmatrix} 1 & 0 \\ 0 & e^{i\pi/4} \end{pmatrix}.$$

It is known that the Clifford gates and the T gate together form a **universal** set of quantum gates—that is, they can construct any quantum computation.

2. Gate Operations in CV Quantum Systems

In most cases, CV systems are modeled using a physical system in which the complex amplitude is quantized. The **annihilation operator**, denoted by $\hat{a}$, is introduced as the quantum operator associated with the classical complex amplitude. This operator decreases the number of particles (in this case photons). Its Hermitian conjugate,[11] $\hat{a}^\dagger$, called the **creation operator**, increases the photon number. For the theoretical background on these operators, refer to Appendix 1.

[11] The Hermitian conjugate of a matrix is defined as the transpose of the matrix with each element replaced by its complex conjugate. The complex conjugate of a number is obtained by reversing the sign of its imaginary part while leaving the real part unchanged.

Here, let us define operators for obtaining the real and imaginary parts of the complex amplitude operator $\hat{a}$ as follows:

$$\hat{x} = (\hat{a} + \hat{a}^{\dagger})/2\,, \hat{p} = -i\,(\hat{a} - \hat{a}^{\dagger})/2.$$

These operators correspond to two continuous-valued physical quantities—position x and momentum p —which serve as the coordinates in phase space. Importantly, they do not commute: $\hat{x}\hat{p} - \hat{p}\hat{x} = i$. Here, non-commutativity implies that the corresponding physical quantities cannot be simultaneously measured with arbitrary precision.[12]

Now, consider the eigenstates of $\hat{x}$ and $\hat{p}$ defined by

$$\hat{x}|x\rangle = x|x\rangle, \hat{p}|p\rangle = p|p\rangle$$

and define the **displacement operator** as

$$\hat{D}(\alpha) = \exp(\alpha\hat{a}^{\dagger} - \alpha^{*}\hat{a}).$$

This operator corresponds to the generation of coherent states (see Appendix 1). This formalism can be used to show the following identities (the detailed calculations are omitted):

$$\hat{D}(s)|x\rangle = \exp(-i2s\hat{p})\,|x\rangle = |x + s\rangle,$$

$$\hat{D}(is)|p\rangle = \exp(i2s\hat{x})\,|x\rangle = |p + s\rangle.$$

That is, $\hat{D}(s)$ and $\hat{D}(is)$ act as **x-displacement and p-displacement gates**, respectively, shifting the coordinates in phase space.

Another important operation is the **quantum non-demolition (QND) gate**, defined as

$$\hat{U}_{\mathrm{QND}}|x\rangle|x'\rangle = |x\rangle|x' + x\rangle.$$

This gate applies a displacement to the second register x' depending on the value of the first. Unlike in DV systems, this gate is a linear transformation with no restriction on the displacement value. Thus, these operations correspond to the Clifford gates and are referred to as **Gaussian operations** in the context of CV-OQC.

In contrast, non-Clifford gate operations in this framework are called **non-Gaussian operations**, which typically include higher-order phase gates, such as the **cubic phase gate**. Mathematically, the cubic phase gate is represented as the unitary transformation,

$$\exp(i\gamma\hat{x}^{3}).$$

---

[12] The operator $\hat{a}$ does not commute, as indicated by the commutation relation $\hat{a}\hat{a}^{\dagger} - \hat{a}^{\dagger}\hat{a} = 1$. Similarly, for the operators $\hat{x}$ and $\hat{p}$, the commutator $\hat{x}\hat{p} - \hat{p}\hat{x} = i$ is non-commutative. In contrast, when the right-hand side is zero (i.e., commutative), the corresponding physical quantities can, in principle, be determined simultaneously with arbitrary precision.

To implement this gate physically, one must realize an interaction that applies the operator $\hat{x}^3$, i.e., evolves the system under a Hamiltonian that contains a cubic term in $\hat{x}$. However, it is currently considered infeasible to realize a strong enough nonlinearity γ by using known physical materials alone. Therefore, implementing universal quantum computations solely through the material-based interactions of CV systems is regarded as extremely difficult. To circumvent this issue, the MBQC approach has attracted increasing attention.

B. Principles of Measurement-Based Quantum Computing

MBQC measures[13] part of the entangled quantum state at specific phase angles and utilizes quantum correlation to induce the desired transformation (computational gate) on the remaining unmeasured part of the state. This operation is performed *adaptively*, meaning that the measurement basis (e.g., measurement angle) for each operation is updated based on the outcome of previous measurements.

Sections III.B.1 and III.B.2 explain the principle of **measurement-based operations** (or **measurement-induced operations**) and how these operations are used to drive the overall process of MBQC. **Quantum teleportation**, described in Appendix 3, provides the basic mechanism underlying MBQC.

1. Quantum Entanglement and Measurement-Based Operations

Quantum entanglement refers to a quantum state in which the measurement outcomes of two quantum systems are correlated. Consider the following representative example of an entangled state:

$$\frac{1}{\sqrt{2}}(|0\rangle_1|0\rangle_2 + |1\rangle_1|1\rangle_2).$$

Here, the subscripts indicate the first and second qubits, respectively. In this entangled state, neither qubit is individually in a definite state of $|0\rangle$ or $|1\rangle$

---

[13] The operation of measurement corresponds mathematically to a projection onto the eigenstates of the operator associated with the measurement. These eigenstates are referred to as the measurement basis. The choice of measurement basis determines which physical quantity becomes definite upon measurement. Moreover, any quantum state that is entangled with the measured state also changes depending on the measurement outcome. For example, the eigenstates of the operator $\hat{\sigma}_z$ correspond to spin-up and spin-down along the z-axis, which remain unchanged under measurements associated with $\hat{\sigma}_z$. However, if a measurement corresponding to $\hat{\sigma}_x$ is performed, the system collapses into the states $|+\rangle$ or $|-\rangle$ with probability 1/2. This property in which a measurement restricts the accessible states is exploited in MBQC.

until measured. However, once one qubit is measured, the other is guaranteed to yield the same outcome. This is one of the **Bell states**, in which two qubits are perfectly correlated (or anti-correlated).

Measuring one qubit of such an entangled state can induce a conditional transformation on the other qubit. An appropriately prepared entangled resource state allows measurements to induce logical operations on the remaining qubit. The measurement outcomes determine known byproduct operations, which can be tracked and correlated classically. This is referred to as a measurement-based operation.

In such operations, the measured qubit is called the **control qubit**, while the qubit upon which the operation is induced is called the **target qubit**. A concrete example of this mechanism is an operation where, if the control qubit is in the $|1\rangle$ state, a unitary operator $\hat{U}$ is applied to the target qubit; if it is in the $|0\rangle$ state, the identity operator $\hat{I}$ is applied instead. This operation is described by the controlled-unitary expression:

$$|0\rangle\langle 0| \otimes \hat{I} + |1\rangle\langle 1| \otimes \hat{U}.$$

Here, $|0\rangle\langle 0|$ and $|1\rangle\langle 1|$ project onto the respective states of the control qubit, and the tensor product $\otimes$ indicates that $\hat{U}$ is applied to the second (target) qubit only if the control qubit is in the $|1\rangle$ state.

This form of conditional operation is analogous to branching logic in classical computing and constitutes a fundamental mechanism in quantum computation.

2. Procedure of MBQC

In MBQC, a large entangled state is first prepared, and then a computation is carried out by successively performing measurements on parts of the entangled stat. Here, we will start by explaining three key features of MBQC.

Distinct computational paradigm: MBQC fundamentally differs from gate-based computing, as described in Section 3.A. In the gate-based model, quantum gates are applied sequentially to qubits, and measurements are performed only at the end to extract the result. Most quantum computing approaches adopt this gate-based model. In contrast, MBQC realizes quantum operations by partially measuring the system and adaptively adjusting the subsequent measurement bases depending on previous measurement outcomes.

Separation of quantum and classical processing: In MBQC, the quantum operations are concentrated in the initial stage in which a large entangled state is generated. Thereafter, the measurement outcomes are treated as classical information to feed back into the system to guide further measurements. Moreover, since errors can be corrected using Clifford operations, MBQC makes it easier to suppress errors arising from manipulation of quantum states.

Universality with fixed entangled resources: In the gate-based model, the quantum circuit must be tailored for each specific computational task. In contrast, in MBQC, the computation is encoded entirely in the classical feedback logic that determines how measurement outcomes influence future measurement bases. Therefore, one can prepare a universal entangled resource state in advance, independent of the specific problem to be solved. Additionally, the structure of the entangled state need not be specialized—any uniformly entangled state suffices as long as it has the necessary correlations.

The CV-OQC approach is particularly well-suited to MBQC because it allows for the physical generation of large-scale entangled states with relative ease.

Next, we explain the overall structure of MBQC by contrasting it with measurement-based operations. Figure 3 illustrates the difference between the two. Both approaches rely on the principle that measuring one quantum state induces an effect on the remaining quantum state. The key distinction is that in MBQC, the outcome of one measurement influences the basis of the next measurement. Although the measurement outcomes are inherently probabilistic, one can effectively implement the desired quantum operation by updating the measurement basis based on previous outcomes.

Figure 3 Measurement-Based Operations and MBQC

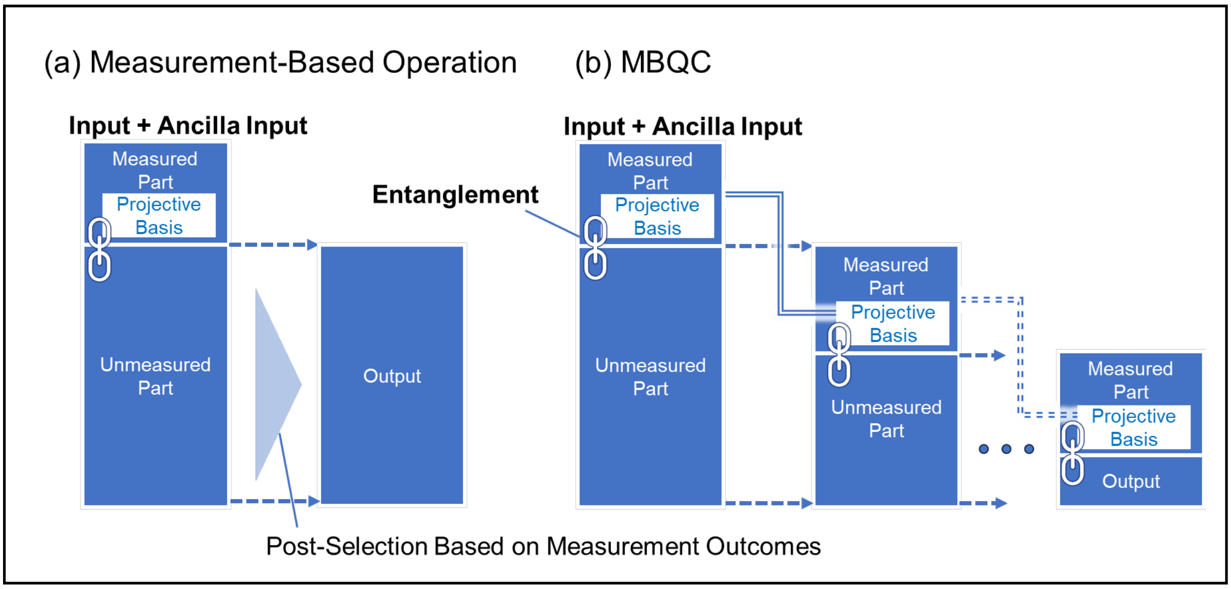

An illustrative example of the overall computational flow in MBQC is shown in Figure 4. First, a large-scale and densely connected entangled quantum state, known as a **cluster state**, is prepared. Next, parts of the state that are not necessary for the desired computation are measured and removed, leaving behind a **graph state** or **entanglement network**. After this, the quantum computation proceeds by sequential and adaptive measurements of the quantum states of the entanglement network. In this process, each measurement outcome is fed forward to and has an effect on the subsequent computational steps. In addition, quantum teleportation may be employed, as needed. By performing a series of these operations, the desired computational result is embedded in the final remaining quantum state. It is known that this procedure can be used to perform any quantum computation—that is, any unitary transformation—making MBQC computationally equivalent to the gate-based quantum circuit model.

Figure 4 Conceptual Illustration of MBQC

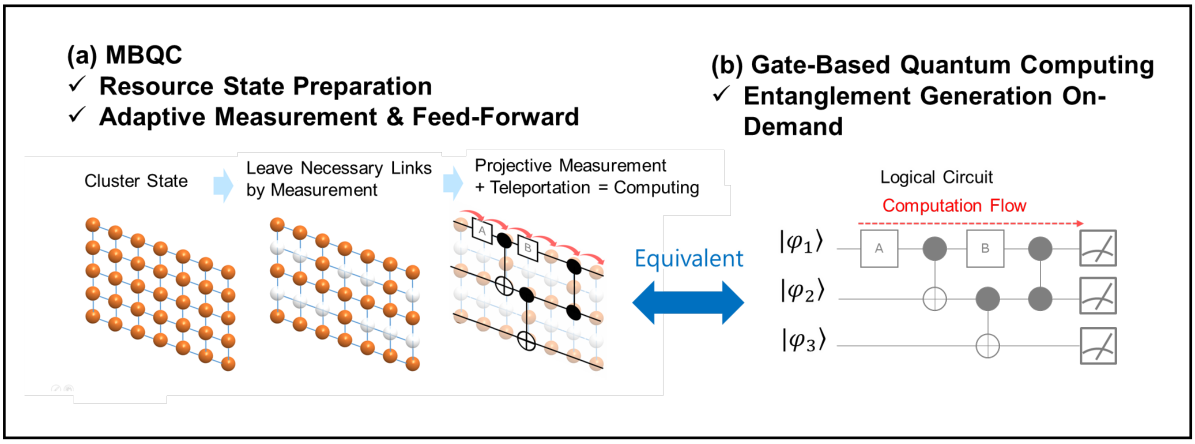

In MBQC, the choices of measurement bases play a role analogous to the specification of gate operations in gate-based quantum computing. The specific way in which these bases are chosen is determined by both the structure of the initial entangled resource (i.e., the graph state) and the target unitary operations to be implemented. Although the technical details are beyond the scope of this paper, readers interested in the concrete construction of such computational schemes are encouraged to refer to standard references such as Koshiba, Fujii, and Morimae [2017].

C. GKP Codes and Gate Operations

Physical quantum states are inherently susceptible to noise. Such noise may originate from environmental factors such as thermal fluctuations, or it may be introduced by quantum operations. In particular, quantum computations may accumulate noise exponentially with respect to the number of operations they entail, making it infeasible to obtain stable computational outcomes through noise suppression techniques alone. Therefore, quantum error correction is essential for performing large-scale computations.

Various methods of quantum error correction have been proposed (see, for example, Nielsen and Chuang [2010] for a comprehensive overview). In both classical and quantum domains, error correction via encoding involves constructing logical bits (or qubits) that exhibit digital (threshold-based) behavior by using multiple physical bits. For instance, in the classical case, a logical bit "0" might be represented by three physical bits "000." If noise causes one of the bits to flip (e.g., "001"), the inconsistency among the bits signals an error, and a majority vote can be used to restore the original state to "0."

In the quantum case, however, directly measuring a qubit to detect errors alters its state. To address this issue, additional qubits are introduced to form entangled states, and certain stabilized subspaces are used for encoding. These code subspaces are spanned by the eigenstates of specific operations (observables) that leave the encoded state invariant. When an operation is applied and the resulting state deviates from the expected invariant form, it is interpreted as an error, which can then be corrected. In mathematics, such operations are known as **stabilizers**, and by combining multiple stabilizers, one can systematically perform encoding, error detection, and error correction. In quantum systems, logical qubits must be encoded using multiple physical qubits to enable fault-tolerant operation. However, this encoding method presents practical difficulties: performing logical operations on such encoded qubits typically requires manipulating all constituent physical qubits simultaneously. This leads to challenges in terms of controllability and noise management.

In CV systems, a single quantum state can encode an amount of information equivalent to many qubits. This allows error-correcting codes to be used without requiring multiple physical qubits. As a result, operations on a logical qubit can be implemented as operations on just one physical quantum state. This is considered one of the key advantages of CV systems.

GKP code is regarded as a promising error-correcting code for CV optical quantum states. The central idea of GKP code is to construct a quantum state in which the probability distribution is concentrated at regular lattice points in the complex amplitude plane—analogously to a Dirac comb in one dimension—and to detect and correct errors by identifying deviations from those lattice points. In this way, a quantum state remains invariant under displacements by integer multiples of a lattice spacing d, which makes such displacements act as stabilizers. Here, let us express the real and imaginary parts of the complex amplitude operator $\hat{a}$ as

$$\hat{x} = (\hat{a} + \hat{a}^{\dagger})/2\,, \hat{p} = -i\,(\hat{a} - \hat{a}^{\dagger})/2.$$

Translations in the real part correspond to the x-direction displacement operator,

$$\widehat{D}_x(s) \overset{\text{def}}{=} \widehat{D}(s) = e^{is\hat{p}},$$

and in the imaginary part to the y-direction displacement operator,

$$\widehat{D}_y(s) \overset{\text{def}}{=} \widehat{D}(is) = e^{is\hat{x}}.$$

Using these operators, a state formed by superposing displaced copies of a reference state over a two-dimensional lattice can be written as

$$\sum_{n_x,n_y} \widehat{D}_x(n_x d)\widehat{D}_y(n_y d)\,|\text{origin}\rangle.$$

This state *appears* to be invariant under lattice translations and hence may seem to be a good encoded state. However, due to the non-commutativity of $\hat{x}$ and $\hat{p}$, namely $\hat{x}\hat{p} - \hat{p}\hat{x} = i$, the displacement operators themselves also do not commute. Here, the general relation[14] between displacement operators is

$$\widehat{D}(\alpha)\widehat{D}(\beta) = e^{\alpha\beta^* - \alpha^*\beta}\widehat{D}(\alpha+\beta).$$

Applying this to lattice translations yields:

$$\widehat{D}_x(n_x d)\widehat{D}_y\left(n_y d\right) = e^{id(n_x\hat{p}+n_y\hat{x})}\left(e^{id^2/2}\right)^{n_x n_y}.$$

This implies that, unless d is carefully chosen, the phases at each lattice point will vary, breaking the stabilizer condition.

However, if the displacement satisfies $e^{id^2/2} = 1$, then the phase becomes invariant. This condition is met when $d = 2\sqrt{\pi}$, in which case the resulting quantum state defines a **GKP code state**.

One practical challenge in using such ideal GKP states is that they consist of infinitely many lattice points extending across the complex plane. **Ideal** GKP states contain points of infinite amplitude and thus require infinite energy, making them physically unrealizable. In practice, therefore, **truncated** GKP states are used, where the lattice points are restricted to those near the origin. The truncated GKP states obey the uncertainty principle, and the probability distributions around each lattice point are broadened accordingly. The distributions are also broadened by imperfections in the physical preparation of the states. Research on using such realistic states for error correction is ongoing, both at the theoretical and experimental levels. On the theoretical side, one promising idea involves constructing hierarchical encodings using multiple imperfect GKP states to form more robust error-correcting codewords. This would allow some degree of imperfection to be tolerated. By contrast, the current experimental realizations are more limited with the most advanced demonstrations having used **Schrödinger cat states**[15] to create one-dimensional

[14] This relationship is derived by noting that the displacement operator forms a Heisenberg Weyl group.

[15] In general, the Schrödinger cat state refers to a quantum superposition of a "live" and a "dead" cat and is frequently cited in quantum mechanical thought experiments. Here, it refers

GKP-like states with only about three peaks in the probability distribution (Konno *et al.* [2024]). Realizing full GKP states requires strongly nonlinear operations, which remain a significant technical challenge for CV-OQC.

specifically to macroscopic entangled states. In quantum optics, this typically indicates a superposition of coherent states with opposite phases. For details, see Appendix 2.

IV. Device Technologies for CV-OQC

This section outlines the device technologies for CV-OQC. Here, **squeezed light** plays a central role. In particular, entangled light pulses are created by passing pairs of squeezed light pulses through beam splitters (see Appendix 4 and Figure 5). A large-scale entanglement is realized by cascading multiple beam splitters, enabling MBQC. This cascaded configuration forms the fundamental architecture of a CV-optical quantum computer. In the sections below we will overview the physical architecture and devices used in it.

A. Architecture of CV Optical Quantum Computers

Figure 5 illustrates one possible configuration of a CV-OQC. The system consists of four main components: a squeezed light generation unit, a cluster generation unit, a quadrature measurement unit, and a measurement control unit.

Figure 5 Architecture of a CV Optical Quantum Computer

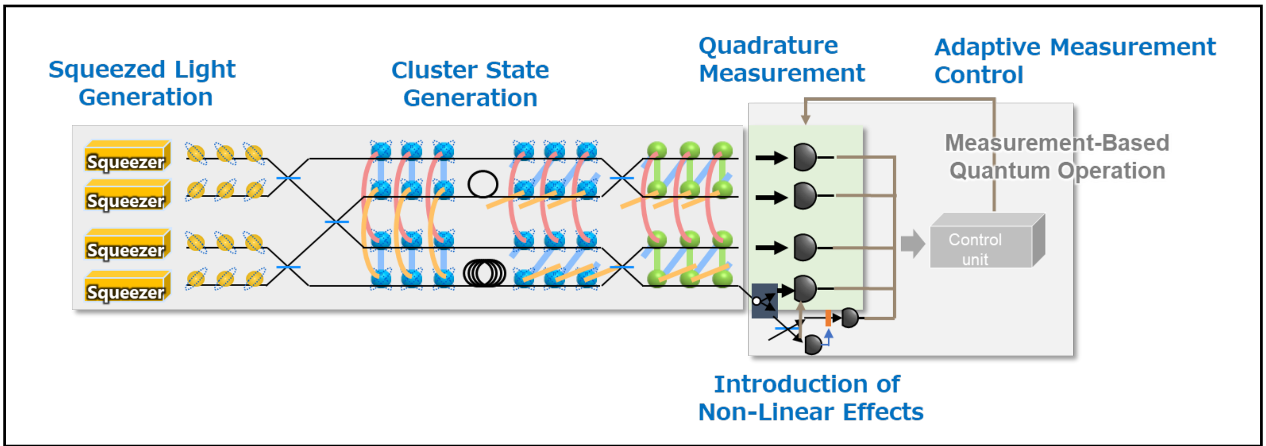

The **squeezed light generation unit** comprises four squeezers—devices that generate squeezed light. These are organized into two pairs, with each pair producing squeezed light along orthogonal directions. The circles adjacent to the squeezers in the figure represent optical pulses, while the ellipses illustrate the spatial compression and expansion in phase space indicative of squeezed states. The technical details of the squeezers are provided in Section IV.D.

The **cluster generation unit** uses beam splitters (depicted as horizontal bars or half mirrors in the diagram) to generate quantum entanglements from the squeezed light. The system involves four optical paths. In the first stage, two pairs of squeezed light pulses are sent through beam splitters to generate initial entanglement. In the next stage, one beam from each pair is further passed through another beam splitter, resulting in a global entanglement of the pulses across all four optical paths.

Subsequently, one optical path from each of the two pairs is delayed—one by a single pulse interval, and the other by N pulse intervals, where N is selected according to the desired size of the generated cluster state. These delayed paths are again combined via beam splitters to further enhance entanglement. This configuration is only one possible example; the location and delay values of the beam splitters and delay lines can be tuned to modify the entanglement structure within the cluster state.

The **quadrature measurement unit** obtains the quantum state information by detecting the real and imaginary parts of the complex amplitudes defined by the phase of the local oscillator. This measurement process is known as **quadrature measurement via homodyne detection**. For details on homodyne detection, see Section IV.C. The four outputs obtained from this stage entangle with pulses in the previous and next time slots via the 1-pulse and N-pulse delays, respectively, forming a two-dimensional entangled network.

The **measurement control unit** dynamically adjusts the measurement basis (e.g., the phase of the local oscillator used in homodyne detection) by using the measurement outcomes of the pulses, thereby enabling adaptive control. This dynamic projection—implemented through modifications in the measurement reference phase—realizes operations on the quantum state.

The lower-right part of Figure 5 conceptually represents a means of introducing nonlinear effects through measurement-based operations, which are under active investigation. The technical specification of this portion is not yet finalized. The figure illustrates an auxiliary quantum state that is prepared via, for example, photon-number-resolving detection, and subsequently used in **quantum teleportation** (see Appendix 3).

B. Photonic Devices Used in CV Optical Quantum Computers

This subsection introduces the individual device components that make up a CV-OQC. At the core of the system are **squeezers**, which act as light sources, and **homodyne detectors**, which perform quadrature measurements and serve as receivers. These elements are connected by **optical paths**—forming a system architecture that closely resembles that of a classical optical communication system. Early OQC studies employed short-wavelength light (around 800 nm), where quantum effects are more pronounced. However, advances in recent years have enabled the use of long-wavelength light in the 1,500 nm telecom band, facilitating the integration of a wide range of communication technologies into OQC. Table 2 summarizes the correspondences between the devices used in communication systems and those in quantum computing. The remainder of this subsection follows the structure of this table to describe each optical device.

Table 2 Correspondence of Device Technologies

	Optical Fiber Communication	CV Quantum Computer
Operation	Digital coherent transmission (Compensating for Large Dispersion)	**MBQC (Computation Using Large-Scale Entanglement)**
Space	Coherent Light × Quadrature Amplitude	**Squeezed Light** × Quadrature Amplitude
Light Source	Coherent light source (Laser)	**Quantum Light Source (Squeezed Light Source)**
Modulation/Gate	Quadrature Amplitude Modulator Beam Splitter Phase Shifter Displacement	CV Quantum Gates Beam Splitter Phase Shifter Displacement **Squeezing** **Cubit Phase Gate**
Detection	Quadrature Amplitude Detection	Quadrature Amplitude Measurement

Red bold: Key differences from optical fiber communications.

Optical communication systems form the backbone of today's information infrastructure, with ongoing advancements in high-capacity transmission technologies. In particular, **digital coherent transmission**, which encodes data in the real and imaginary components (in-phase and quadrature amplitudes) of coherent light, has become mainstream. On the **transmitter side**, data is encoded onto a coherent laser beam via quadrature amplitude modulation. On the **receiver side**, quadrature amplitude detection is performed by interfering the signal with a **local oscillator** (**LO**)[16] and its 90-degree phase-shifted counterpart. This process enables the extraction of the encoded data without requiring precise phase or frequency synchronization between the transmitter and receiver. Advanced **adaptive equalization filters** correct distortions caused by dispersion

[16] LO light refers to the local oscillator, a reference light used in optical measurement technologies.

or pulse deformation during transmission. For instance, dispersion over a 100-km fiber transmission can broaden a 100 Gbaud[17] signal by a factor of 1,000. In such case, the receiver must reconstruct the signal by distinguishing its components that have been spread out over thousand pulses.

Many of these classical optical communication techniques can be adapted to OQC. For simplicity, this subsection uses **communication systems** to refer to classical systems and **quantum systems** to refer to CV-OQC. In **communication systems**, adaptive equalization is used to restore signals distorted across multiple pulses, even when the receiver lacks prior knowledge of the transmitter's polarization or phase (analogous to a quantum basis). In contrast, **quantum systems** use entangled optical pulses to dynamically modify the measurement basis during a computation. Here, the quantum analogue of transmitter-side modulation is dynamic control of the measurement basis—implemented by adjusting the LO in quadrature measurements.

While both domains embed information into the real and imaginary parts of the light's amplitude, the key distinction lies in the type of light used: coherent light in **communication systems** and squeezed, entangled light in **quantum systems**. Coherent and squeezed states are generated using laser sources and squeezers, respectively, and act as carrier waves[18].

For signal generation in **communication systems**, signal modulation is applied to the amplitude of the carrier. In **quantum systems**, operations involve generating GKP-coded states within pulses or dynamically changing measurement bases by using previous measurement outcomes. Classical optical elements such as beam splitters and phase shifters are reused as quantum gates. However, quantum computing also requires operations like squeezing and cubic phase gates, the latter of which currently lack a practical physical implementation due to the difficulty of achieving strong third-order nonlinearities. As a result, quantum teleportation-based substitutes[19] are under investigation.

Signal recovery (in **communication systems**) and measurement (in **quantum systems**) both rely on quadrature amplitude detection. A key

[17] A gigabaud (Gbaud) is a unit of symbol rate in data communications, representing the transmission of one billion symbols per second. One baud corresponds to the transmission of one symbol per second.

[18] A carrier wave is a reference waveform used to transmit information.

[19] Although no optical component capable of directly implementing nonlinear operations such as a cubic phase gate has been discovered, methods utilizing quantum teleportation have been proposed to indirectly induce such nonlinear effects (see Miyata *et al.* [2016]).

difference lies in frequency matching: **communication systems** often use **intradyne detection**[20] because of difficulties in frequency alignment between the LO and the carrier, whereas quantum systems typically use homodyne detection where the LO and carrier are phase-locked.

The relationship between communication and quantum technologies is mutually beneficial and expected to yield significant synergies. For example, homodyne detection techniques developed for quantum applications could be used in classical communication to reduce the computational overhead of digital signal processing in intradyne detection. Conversely, high-speed optical modulation and reception technologies developed for communication could dramatically reduce the pulse width from the current 10 nanoseconds to as short as 1 picosecond, enabling scaling up of the size of computations performable with quantum systems.

The following subsections introduce three key optical device technologies: coherent detection techniques, integrated waveguide circuits, which are linear optical components, and periodically poled lithium niobate (PPLN)-based squeezers.

C. Optical Devices for Detection of Coherent States

The physical techniques for generating, transmitting, and detecting coherent light are well established as **coherent detection technologies** in classical optical fiber communication (see Kikuchi [2009]). In optical fiber communication, information is transmitted by modulating the in-phase (cosine) and quadrature (sine) components of a coherent light wave over time. On the receiving side, the incoming optical signal is split into two paths. One is interfered with a LO light source, and the other with a 90-degree phase-shifted version of the LO. By measuring the intensities of these interference signals, one can obtain both the in-phase component (which is in phase with the LO) and the quadrature-phase component (which is 90 degrees out of phase with the LO). These signals are then processed using digital signal processing techniques to extract the modulated frequency components and apply adaptive equalization, thereby recovering the original transmitted information.

[20] Intra-dyne detection is a form of coherent detection used when the frequency offset between the local oscillator and the carrier wave is very small. While homodyne detection requires the frequency difference to be exactly zero, intra-dyne allows for small deviations, offering greater tolerance in practical systems.

In CV-OQC, a similar detection technique known as **homodyne detection** is employed, in which the signal and LO light have matching frequencies. Despite the quantum context, the core idea—extracting complex amplitude information from light—is fundamentally the same. Furthermore, the detection of squeezed light can also be achieved by adapting coherent light detection techniques. In homodyne detection, the intensity of the interference between the signal and the LO provides direct access to the cosine and sine components of the optical field without any filtering, enabling the quantum state to be observed on a macroscopic level.

This transfer of technology from communication to quantum computing can also be viewed as ways of leveraging the phase space representation of coherent states in terms of their in-phase and quadrature components. This correspondence between classical and quantum states within the same phase space enables classical technologies and devices developed for optical communications to be directly applied to quantum information processing. This in turn explains why many classical optical technologies can be repurposed for use in OQC and why this cross-disciplinary synergy has already produced significant results.

D. Linear Optical Elements and Integrated Circuits

In optical communications, **optical waveguide circuits** are used as integrated optical circuits. These circuits are fabricated from various materials, with silica-based planar lightwave circuits being commonly used for their low optical loss. These circuits are manufactured using a combination of optical fiber fabrication techniques and semiconductor microfabrication technologies, allowing the integration of components such as directional couplers for optical splitting and interferometers. By combining these components, devices such as interferometers and displacement elements (in this context, optical combiners for signals of the same frequency) can be integrated onto a single chip (Masada *et al.* [2015]).

Figure 6 shows an example of an integrated circuit that consolidates the functions required to realize quantum teleportation. The circuit includes functionalities for generating quantum entanglement and performing Bell basis transformations using directional couplers. It also integrates circuits for combining LO light and signal light, which is essential for making quadrature measurements. Furthermore, this circuit works in conjunction with photodetectors to perform quadrature measurements. The measurement outputs can then be fed into a displacement element to manipulate the optical state accordingly.

Figure 6 Optical Circuit Integrating Linear Optical Elements

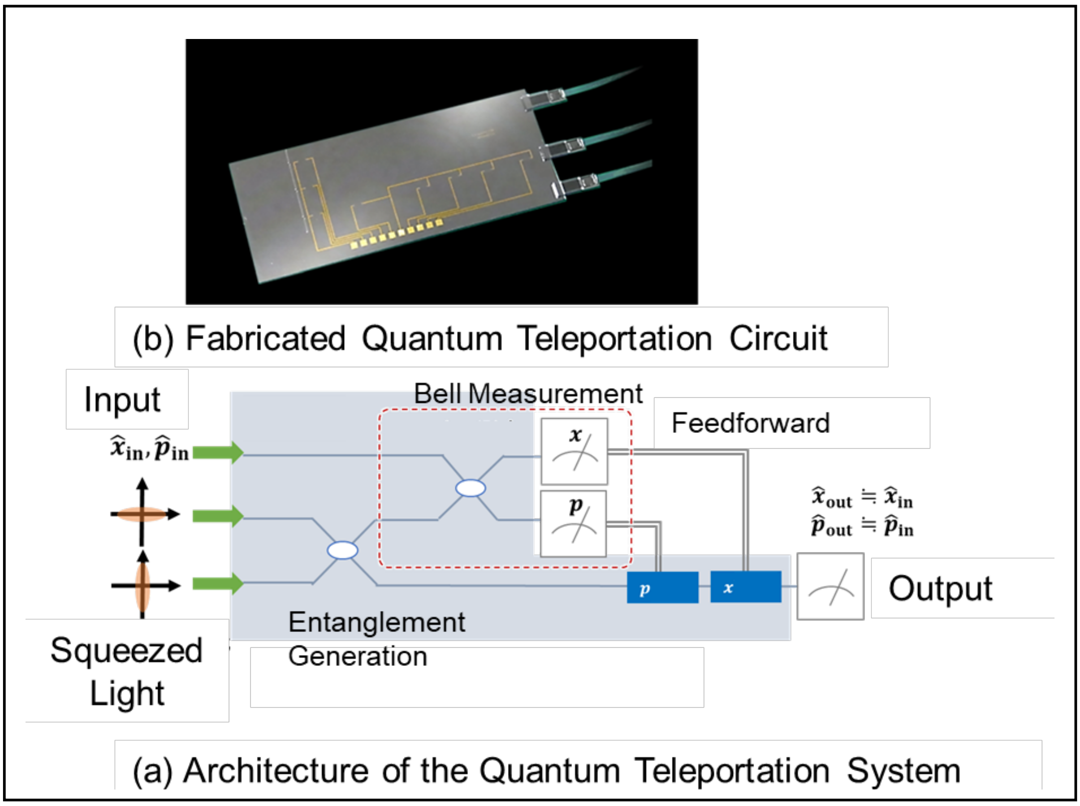

Currently, free-space optical systems [21] are predominantly used in CV optical quantum computers in order to minimize loss to the greatest extent possible. Furthermore, as technologies for reducing loss continue to advance, it is expected that they will enable more compact system designs and improved phase-locking stability of integrated optical circuits such as those described above.

E. Squeezed Light Sources Using PPLN

PPLN is a nonlinear optical medium created by periodically in space inverting the polarization of lithium niobate ($LiNbO_3$), which exhibits second-order

[21] A free-space optical system refers to a system where optical pulses are transmitted through the atmosphere rather than through optical fibers for communication.

nonlinearity. This periodic poling enables quasi-phase matching, allowing efficient generation of nonlinear optical phenomena.

PPLN facilitates second-order nonlinear effects, such as **second harmonic generation** and **difference frequency generation**, where the refractive index changes in response to the optical intensity. In particular, **phase-sensitive amplification** has attracted attention for enabling noiseless optical amplification, and has been researched in optical communications.

To enhance amplification efficiency, the optical intensity must be increased by confining light in a narrow region to boost the nonlinear interaction. To this end, stripe-shaped waveguide structures fabricated with micrometer-scale precision (see Figure 7) have been developed. Currently, optical amplification factors exceeding 1,000 times have been achieved, making these devices promising for practical optical communication systems. When such a PPLN waveguide is used as an optical parametric down-converter, it can generate highly squeezed light (Kazama *et al.* [2021]).

Figure 7 Squeezer Based on PPLN Waveguide

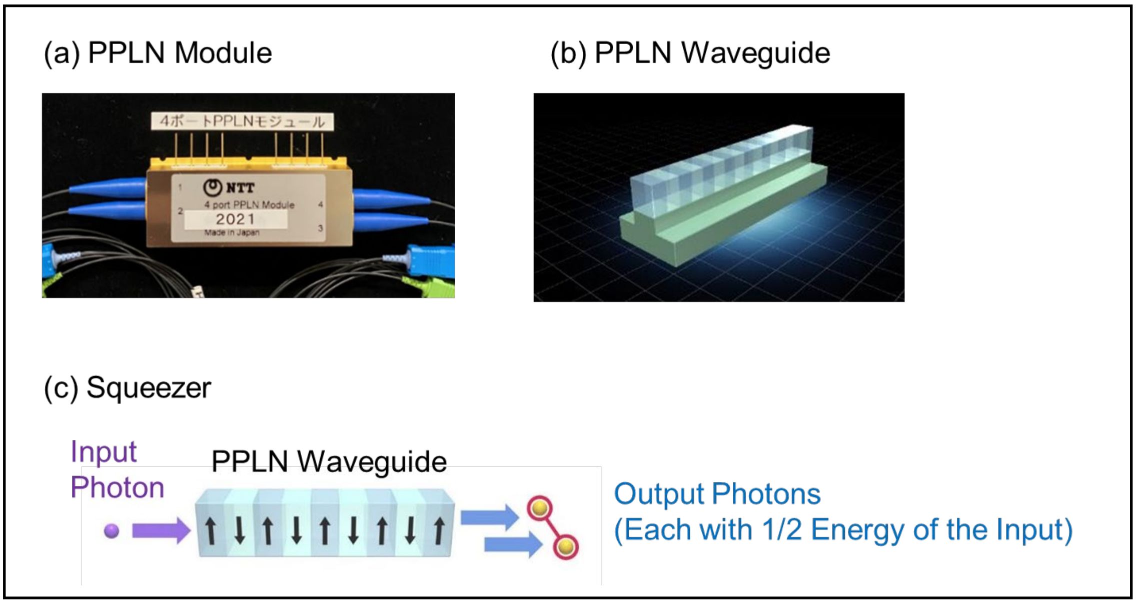

One important metric that characterizes the quantum nature of squeezed light is the **squeezing level.**[22] Achieving a higher squeezing level requires

[22] The squeezing level quantifies the degree to which quantum fluctuations are compressed in squeezed light. It is expressed as the ratio between the variances in the broadened and narrowed quadratures and is typically measured in decibels (dB).

minimizing optical losses during conversion. In this respect, PPLN waveguides enable high conversion efficiency over short propagation lengths, which in turn reduces loss and facilitates the generation of squeezed light with higher squeezing levels. Other schemes that require optical cavities for resonant enhancement restrict the frequency of the squeezed light to the cavity modes. In contrast, PPLN waveguides do not rely on optical resonance, thereby enabling squeezed light to be generated over a broad frequency bandwidth.

This broadband squeezing increases the speed of quantum information processing by enabling short optical pulses to be synthesized from multiple frequency component. Current PPLN waveguides have demonstrated squeezing levels of approximately 8 dB over bandwidths up to 10 THz. However, support for large-scale entanglements, quantum teleportation, and GKP code state generation is believed to require squeezing levels of at least 10 dB. Efforts are underway to improve device characteristics and reach this threshold.

V. Challenges and Recent Developments in CV Optical Quantum Information Processing

This section outlines the current status of CV-OQC technologies and organizes the key challenges in the field. While the foundation of CV-OQC has been laid by integrating well-established optical communication technologies with fundamental research into optical quantum information processing, the realization of scalable and fault-tolerant quantum computing remains a distant goal, much like in other quantum computing approaches. Scalability and fault tolerance are not independent challenges, but rather interdependent requirements that must be addressed simultaneously. The fundamental research continues on devising ways to meet both requirements. In the following, we review the current state of research and development at major companies and research institutions.

A. Current Status of CV Optical Quantum Computer Development

Xanadu, a Canadian company, is actively developing a commercial CV-OQC architecture. Like other firms in the field, Xanadu aims to build a general-purpose quantum computer (Bourassa *et al.* [2021]). As a major milestone, the company reported in 2022 that its device had achieved a quantum advantage in solving a sampling problem known as Gaussian Boson Sampling[23] (GBS, Madsen *et al.* [2022]).[24] The system is commercially available under the name "Borealis". In 2025, Xanadu announced "Aurora", a modular optical quantum computer comprising 35 photonic chips interconnected by optical fibers and housed in server racks. In principle, this system supports computations with up to 12 GKP-encoded qubits. However, only a limited portion of the system has been experimentally verified, and the error correction using the GKP-encoded qubits has not yet been implemented. While the company's website details theoretical methods for realizing fault-tolerant GKP code states, these remain largely

[23] The boson sampling problem involves predicting the output distribution of a quantum circuit when single photons are input. Although it lacks immediate applications, its computational difficulty for classical systems and relative ease for quantum computers make it a benchmark for determining quantum advantage. Due to the difficulty of generating stable single photons, the GBS problem, in which squeezed states are used instead, is employed in CV optical quantum systems.

[24] Specifically, entanglement across 216 distinct quantum states referred to as Qu-modes are generated by passing a sequence of squeezed light pulses through pairs of delay lines (with 6-pulse and 36-pulse delays). These Qu-modes are distributed among 16 output channels, and sampling is performed using photon-number-resolving detectors.

conceptual. The central bottleneck is the lack of efficient physical implementations of GKP states. Notably, a new scheme for more efficient GKP code state generation has been proposed through collaborative research between the University of Tokyo (Furusawa Lab) and Xanadu's development team (Takase *et al.* [2024]), raising expectations for a future experimental realization.

The **University of Science and Technology of China** is also pursuing GBS-dedicated optical quantum computers. In 2020, the group reported a demonstration of quantum advantage using such a device (Zhong *et al.* [2020]) and since have made system upgrades and further claims of quantum advantage (Zhong *et al.* [2021], Chen *et al.* [2023]).

In Japan, the **RIKEN OQC Research Team**, led by Prof. Akira Furusawa, started the development of a fault-tolerant, large-scale general-purpose optical quantum computer, based on MBQC. Research on generating cluster states[25], the computational resources for MBQC, is being conducted by the University of Tokyo and the Technical University of Denmark. Their studies have demonstrated large-scale optical-cluster-state generation (Larsen *et al.* [2019], Asavanant *et al.* [2019], Takeda, Takase, and Furusawa [2019]), and they have successfully performed actual quantum computations using these cluster states (Larsen *et al.* [2021], Asavanant *et al.* [2021]). Moreover, RIKEN has launched the world's first cloud-accessible optical quantum computer capable of performing linear computations across approximately 100 quantum modes (optical pulses). Their roadmap envisions expanding this platform into a universal quantum computer by introducing nonlinear operations and GKP-based encoding of quantum modes.[26]

To this end, measurement-based nonlinearities are under investigation at the University of Tokyo. Key achievements include experimental demonstrations of nonlinear measurement-based operations (Sakaguchi *et al.* [2023]) and approximate GKP state generation via measurement-based techniques, as initially proposed (Konno *et al.* [2024]). As an alternative to cluster-state-based MBQC, researchers are also exploring a loop-based OQC architecture, in which measurement-based quantum gates are applied sequentially. This approach has

[25] Cluster states are special multiparticle entangled states that enable arbitrary quantum gate operations through relatively simple procedures. Their usefulness has attracted increasing attention in recent years.

[26] https://www.riken.jp/pr/news/2024/20241108_2/index.html

been experimentally validated in a series of studies (Takeda and Furusawa [2017]; Enomoto *et al.* [2021]; Yonezu *et al.* [2023]; Yoshida *et al.* [2025]).

B. Technical Challenges

1. Modeling of Quantum States

A key challenge in achieving fault-tolerant quantum computing lies in the theoretical modeling of the quantum states themselves. As noted in Section III.C., the GKP code state theoretically has the probability amplitudes at all lattice points in phase space, implying that infinite energy would be needed for a physical realization. However, real-world systems must operate under finite energy constraints. Thus, only a finite subset of lattice points, typically those near the origin, can be used to approximate GKP code states. The modeling strategy for GKP code states directly affects all aspects of a quantum computing system, including the theoretical performance requirements and the achievable physical performance of its devices.

2. Improvements to Physical Device Performance

The squeezing level[27] determines the fault tolerance of GKP code states, i.e., the acceptable error rate for logical qubits. The initial proposal of GKP error correction (Gottesman, Kitaev, and Preskill [2001]) indicates that achieving an error threshold of 2×10^{-2} would require a squeezing level of approximately 14.8 dB.

Current device performance falls short of this target. For example, in promising devices like PPLN-based squeezers, even a 0.5 dB optical loss can make it difficult to reach an even 10-dB squeezing level. Since this level of the loss is comparable to the misalignment loss in optical connectors, it implies that extremely high-precision fabrication and alignment technologies are required. Thus, while further improvement in physical performance remains a technical goal, the maturity of current device technologies suggests limited room for improvement. Nevertheless, progress is still expected through advances in fabrication and auxiliary technologies.

3. Easing of Theoretical Performance Requirements

[27] This refers to the squeezing asymmetry index, which quantifies the directional imbalance in quantum fluctuation compression in squeezed light.

Given the limited room for device improvement, easing of the theoretical performance requirements (e.g., squeezing level) through innovations in error correction is regarded as important. According to Fukui, Tomita, and Okamoto [2017], such refinements could lower the squeezing threshold for fault tolerance to around 10 dB. Specifically, one strategy involves building higher-level encoded states on top of GKP-encoded states.

Still, even a 10-dB squeezing level represents a tight margin. Even if devices with such capability are developed, the system as a whole would still lack enough robustness for scaling. Hence, progress must be made in both theory (e.g., threshold reduction) and hardware (e.g., squeezing level enhancement).

4. Development of Hardware Components

To perform universal quantum computation in CV-OQC, the following components are essential (as described in Section IV): 1. squeezers, 2. beam splitters, 3. phase shifters, 4. displacement operators (optical modulators), and 5. cubic phase gates.

Components 2, 3 and 4 are standard in classical optics and are widely used in optical communications. In addition, homodyne detection is typically used for quadrature measurements. However, components 1 and 5 go beyond conventional optical communications and involve technologies used in a few other cutting edge fields.

Squeezers, which generate squeezed light, play a key role as quantum light sources in CV-OQC; these are analogous to laser sources in optical communications. As noted in Section IV.C, parametric amplifiers,[28] originally designed for optical communications, have been repurposed to create efficient squeezers. PPLN waveguides offer world-class performance, achieving 8 dB squeezing levels and 10 THz bandwidths. Similarly to their use in optical communications, their wide bandwidth enables many quantum pulses to be multiplexed and used for large-scale quantum computations. Indeed, squeezers have been demonstrated to generate arbitrary quantum states in time bins.

[28] Parametric amplification is an amplification method that utilizes nonlinear media to generate signal components proportional to the product of optical amplitudes. The product of two sine waves, such as $\sin\omega_1 t \times \sin\omega_2 t = \frac{1}{2}(\cos(\omega_1 - \omega_2)t - \cos(\omega_1 + \omega_2)t)$, results in a combination of cosine waves at the sum and difference frequencies. This principle enables the generation of laser light at desired wavelengths from multiple input beams.

The cubic phase gate is particularly challenging, as it is a non-Clifford gate and yet is crucial for achieving a universal quantum computer. While operations 1–4 correspond to Clifford gates, the cubic phase gate lies beyond current device capabilities. As a workaround, methods using non-Gaussian quantum measurements via quantum teleportation have been proposed (e.g., Miyata *et al.* [2016]), and their experiments are anticipated.

5. Development of Control Circuits

In order to orchestrate these hardware components into a unified quantum computing system, control circuits for managing optical devices are essential. If the quantum state of each optical device can be measured with sufficient precision, feedback control becomes possible. Such control could benefit from advancements in digital control over analog signals, including technologies such as jitter suppression.[29]

Another major technical challenge is the clock speed of control circuits. Current systems operate at around 100 MHz, whereas the optical carrier frequency is approximately 200 THz—a disparity of a factor of one million. To bridge this gap, 100-GHz signal generators, commonly used in modern optical communications, could be repurposed for quantum computing. This would dramatically increase the computational throughput per unit time. Furthermore, if optical control of circuits becomes feasible (i.e., controlling operations with light rather than electronics), operations in the terahertz regime may be achievable, enabling even higher processing speeds.

However, developing such control circuits requires integrated hardware-software co-design and must draw upon expertise from multiple disciplines. This implies the need for large-scale collaborative projects involving research institutions and industry partners with complementary technical strengths.

[29] Jitter refers to the fluctuation in the timing of digital signals. Excessive jitter degrades signal integrity, making its control and suppression critical for high-speed data processing and large-capacity communications.

VI. Conclusion

The CV-OQC approach, which is inherently robust against thermal noise at room temperature, is a promising candidate for realizing low-cost quantum computing. The development of this approach can build upon the accumulated technologies in optical communications. For example, wavelength-division multiplexing technique could be used to scale up quantum computing systems. On the other hand, there remain challenges unique to this approach. In particular, it is essential to address critical issues regarding feasibility and stability of system implementations. Although long-term efforts will be required to overcome the issues, the research in this field is also expected to bring about secondary benefits.

First, CV-OQC technologies are expected to contribute to other quantum computing approaches. In approaches such as superconducting qubits, neutral atoms, and trapped ions, where large-scale integration or long-distance interconnection of systems is required, light serves as a promising medium for transmitting quantum information. In this context, techniques for encoding and transmitting quantum information using light may offer valuable contributions.

Furthermore, the technologies developed for CV-OQC can also be applied to optical communications. Optical quantum computers employ the high-precision coherent detection method known as homodyne detection. If homodyne detection can be applied to optical communications, it may enable much more data to be transmitted while reducing the computational cost of digital signal processing.[30] One of the challenges to using homodyne detection for communications is the distribution of optical reference signals, which serve as clock signals in classical systems. This challenge may be resolved in parallel with advancements in OQC technologies. Just as GPS (Global Positioning System) signals have become a widely used reference across various devices, it is conceivable that optical signals used in homodyne detection will, in the future, become standardized as a common foundational technology in society.

In conclusion, although numerous challenges remain regarding the feasibility and ultimate architecture of quantum computers, the CV-OQC approach stands out as a strong candidate. Moreover, the technologies developed for CV-OQC are expected to be useful in other quantum computing approaches.

[30] In digital coherent transmission systems used in optical communications, intra-dyne detection techniques are commonly employed. In this scheme, it is not necessary for the frequency of the reference light (local oscillator) and that of the signal light to match exactly; detection and signal recovery are performed under the condition that their frequencies are approximately equal.

Thus, continued research and development on CV-OQC involving collaborations combining the complementary strengths of the public sector and private enterprises will be invaluable.

References

Asavanant, Warit, Yu Shiozawa, Shota Yokoyama, Baramee Charoensombutamon *et al.*, "Generation of Time-Domain-Multiplexed Two-Dimensional Cluster State," *Science*, 366(6463), 2019, pp. 373—376.

——, Baramee Charoensombutamon, Shota Yokoyama *et al.*, "Time-Domain-Multiplexed Measurement-Based Quantum Operations with 25-MHz Clock Frequency," *Physical Review Applied*, 16(3), 034005, 2021.

Bourassa, J. Eli, Rafael N. Alexander, Michael Vasmer *et al.*, "Blueprint for a Scalable Photonic Fault-Tolerant Quantum Computer". *Quantum*, 5, 392, 2021.

Chen, Ming-Cheng Chen, Jian Qin, Li-Chao Peng *et al.*, "Gaussian Boson Sampling with Pseudo-Photon-Number-Resolving Detectors and Quantum Computational Advantage," *Physical Review Letters*, 131, 150601, 2023.

Dey, Rukmini, Joseph Samuel, and Rithwik S. Vidyarthi, "Coadjoint Orbits and Kähler Structure: Examples from Coherent States," *Reports on Mathematical Physics*, 89(3), 2022, pp. 267—290.

Enomoto, Yutaro, Kazuma Yonezu, Yosuke Mitsuhashi, Kan Takase, and Shuntaro Takeda, "Programmable and Sequential Gaussian Gates in a Loop-Based Single-Mode Photonic Quantum Processor," *Science Advances*, 7(46), eabj6624, 2021.

Fukui, Kosuke, Akihisa Tomita, and Atsushi Okamoto, "Analog Quantum Error Correction with Encoding a Qubit into an Oscillator," *Physical Review Letters*, 119(18), 180507, 2017.

Gottesman, Daniel, Alexei Kitaev, and John Preskill, "Encoding a Qubit in an Oscillator," *Physical Review A*, 64(1), 012310, 2001.

Kazama, Takushi, Takeshi Umeki, Shimpei Shimizu, Takahiro Kashiwazaki, Koji Enbutsu, Ryoichi Kasahara, Yutaka Miyamoto, and Kei Watanabe, "Over-30-dB Gain and 1-dB Noise Figure Phase-Sensitive Amplification Using a Pump-Combiner-Integrated Fiber I/O PPLN Module," *Optics Express*, 29(18), 2021, pp. 28824—28834.

Kikuchi, Kazuro, "Digitaru Kohirento Hikari Tsushin Gijyutu (Digital Coherent Optical Communication Technology)," *Kogaku (Japanese Journal of Optics)*, 38(5), 2009, pp. 258–262. [In Japanese]

Konno, Shunya, Warit Asavanant, Fumiya Hanamura *et al.*, "Logical States for Fault-Tolerant Quantum Computation with Propagating Light," *Science*, 383(6680), 2024, pp. 289—293.

Koshiba, Takeshi, Keisuke Fujii, and Tomoyuki Morimae, *Kansoku Ni Motoduku*

Ryoushi Keisan (Measurement-Based Quantum Computation), Corona Publishing Co., Ltd., 2017. [In Japanese]

Kuratsuji, Hiroshi, *Kikagakuteki Ryoushi Rikigaku (Geometric quantum mechanics)*, Springer-Verlag Tokyo, 2005. [In Japanese]

Larsen, Mikkel V., Xueshi Guo, Casper R. Breum, Jonas S. Neergaard-Nielsen, and Ulrik L. Andersen, "Deterministic Generation of a Two-Dimensional Cluster State," *Science*, 366(6463), 2019, pp. 369—372.

——, ——, ——, ——, and ——, "Deterministic Multi-Mode Gates on a Scalable Photonic Quantum Computing Platform," *Nature Physics*, 17, 2021, pp. 1018—1023.

Madsen, Lars S., Fabian Laudenbach, Mohsen Falamarzi Askarani *et al.*, "Quantum Computational Advantage with a Programmable Photonic Processor," *Nature*, 606(7912), 2022, pp. 75—81.

Masada, Genta, Kazunori Miyata, Alberto Politi, Toshikazu Hashimoto, Jeremy L. O'Brien, and Akira Furusawa, "Continuous-Variable Entanglement on a Chip," *Nature Photonics*, 9(5), 2015, pp. 316—319.

Miyata, Kazunori, Hisashi Ogawa, Petr Marek, Radim Filip, Hidehiro Yonezawa, Jun-ichi Yoshikawa, and Akira Furusawa, "Implementation of a Quantum Cubic Gate by an Adaptive Non-Gaussian Measurement," *Physical Review A*, 93, 022301, 2016.

Nielsen, Michael A., and Isaac L. Chuang, *Quantum Computation and Quantum Information: 10th Anniversary Edition*, Cambridge University Press, 2010.

Rad, H. Aghaee, T. Ainsworth, R. N. Alexander *et al.*, "Scaling and Networking a Modular Photonic Quantum Computer," *Nature*, 638, 2025, pp. 912—919.

Sakaguchi, Atsushi, Shunya Konno, Fumiya Hanamura *et al.*, "Nonlinear Feedforward Enabling Quantum Computation," *Nature Communications*, 14, 3817, 2023.

Takase, Kan, Fumiy Hanamura, Hironari Nagayoshi, J. Eli Bourassa, Rafael N. Alexander, Akito Kawasaki, Warit Asavanant, Mamoru Endo, and Akira Furusawa, "Generation of Flying Logical Qubits Using Generalized Photon Subtraction with Adaptive Gaussian Operations," *Physical Review A*, 110(1), 012436, 2024.

Takeda, Shuntaro, and Akira Furusawa, "Universal Quantum Computing with Measurement-Induced Continuous-Variable Gate Sequence in a Loop-Based Architecture," Physical Review Letters, 119, 120504, 2017.

——, Kan Takase, and Akira Furusawa, "On-Demand Photonic Entanglement

Synthesizer," *Science Advances*, 5(5), eaaw4530, 2019.
Yonezu, Kazuma, Yutaro Enomoto, Takato Yoshida, and Shuntaro Takeda, "Time-Domain Universal Linear-Optical Operations for Universal Quantum Information Processing," *Physical Review Letters*, 131, 040601, 2023.
Yoshida, Takato, Daichi Okuno, Takahiro Kashiwazaki, Takeshi Umeki, Shigehito Miki, Fumihiro China, Masahiro Yabuno, Hirotaka Terai, and Shuntaro Takeda, "Sequential and Programmable Squeezing Gates for Optical Non-Gaussian Input States," *PRX Quantum*, 6, 010311, 2025.
Zhong, Han-Sen, Hui Wang, Yu-Hao Deng *et al.*, "Quantum Computational Advantage Using Photons," *Science*, 370(6523), 2020, pp. 1460—1463.
——, Yu-Hao Deng, Jian Qin *et al.*, "Phase-Programmable Gaussian Boson Sampling Using Stimulated Squeezed Light," *Physical Review Letters*, 127, 180502, 2021.

List of Symbols

Symbols	Description
$\|a\rangle,\ \langle a\|$	Quantum state vectors. The ket $\|a\rangle$ is a column vector, and the bra $\langle a\|$ is the Hermitian conjugate (complex conjugate transpose) of the ket, represented as a row vector.
$\|a\rangle\langle b\|$	Outer product or dyadic tensor, formed by the matrix product of a ket (column vector) and a bra (row vector).
$\otimes$	Tensor product
$\langle \mathrm{a}\|b\rangle$	Inner product, computed as the matrix product of a bra and a ket, resulting in a scalar.
$\hat{\ }$	The hat symbol denotes a matrix or a quantum operator
Tr	Trace of a matrix, defined as the sum of its diagonal elements, or the total expectation value over an orthonormal basis.
$\hat{a}^{\dagger},\ \hat{a}$	Creation and annihilation operators (also referred to as raising and lowering operators). The dagger $\dagger$ indicates the Hermitian conjugate (complex conjugate transpose). In this context, $\hat{a}$ is the quantized operator corresponding to the amplitude of the electromagnetic wave.
$\hat{x} = \frac{1}{2}(\hat{a}^{\dagger} - \hat{a})$, $\hat{p} = \frac{1}{2}(\hat{a}^{\dagger} - \hat{a})$	Position and momentum operators (in-phase and quadrature-phase operators, respectively). $\hat{x}$ corresponds to the real part of the amplitude, and $\hat{p}$ to the imaginary part.
$\|0\rangle, \|1\rangle$ or $\|\uparrow\rangle, \|\downarrow\rangle$	Basis states of a qubit
$[\hat{A}, \hat{B}]$	Commutator of operators $\hat{A}$ and $\hat{B}$, defined as $[\hat{A}, \hat{B}] = \hat{A}\hat{B} - \hat{B}\hat{A}$. In particular, bosonic modes satisfy the canonical commutation relation $[\hat{a}, \hat{a}^{\dagger}] = 1$.

Appendix 1. Mathematics of CV Optical Quantum States

In DV quantum states, their eigenvalues are discrete. However, in CV quantum states, the eigenvalues take continuous values. Thus, CV quantum states can, where appropriate, be treated in a manner analogous to classical states in which physical quantities assume continuous values. A typical example of such a state is the coherent state.

A. Coherent States

Mathematically, a **coherent state** is described as follows. First, define the skew-Hermitian operator[31] $\alpha\hat{a}^\dagger - \alpha^*\hat{a}$, which is a linear combination of the creation and annihilation operators $\hat{a}^\dagger$ and $\hat{a}$, multiplied by a complex coefficient α. Then, construct the unitary operator $\widehat{D}(\alpha) = \exp(\alpha\hat{a}^\dagger - \alpha^*\hat{a})$.[32]

Applying this operator to the vacuum state $|0\rangle$, which satisfies $\hat{a}|0\rangle = 0$, yields the coherent state $\widehat{D}(\alpha)|0\rangle$.

Although some conditions may be required depending on the context, coherent states possess the property of achieving the minimum uncertainty product within the limits imposed by the uncertainty principle of quantum mechanics. Because they minimize the uncertainty in specific physical quantities, coherent states are regarded as *the most classical* among quantum states.

B. Quantum Harmonic Oscillator of Light

To derive the mathematical description of optical coherent states,[33] we begin with an explanation of the quantum harmonic oscillator, which describes quantized states of light.

Light is a form of electromagnetic wave. When the amplitude of such a wave is quantized, its quantum state can be represented mathematically in the same form as a quantized spring (see Table A1). This formulation is known as the **harmonic oscillator**.

---

[31] Taking the Hermitian conjugate of an operator reverses its sign, depending on the algebraic context in which it appears.

[32] The operator $\widehat{D}(\alpha)$ is referred to as the displacement operator or alternatively as the Weyl operator.

[33] In the case of light, such states are called bosonic coherent states or Weyl-Heisenberg coherent states.

Table A1 Quantization of Light and Its Mathematical Representation

	a	$\frac{1}{\sqrt{2}i}(a+a^{\dagger})$	$\frac{1}{\sqrt{2}i}(a-a^{\dagger})$
Classical State	Complex Amplitude	Real Part (In-Phase)	Imaginary Part (Quadrature-Phase)
CV Optical Quantum State	Annihilation Operator	Position Operator x	Momentum Operator p
		Measured by Homodyne Detection	

In quantum mechanics, the operator corresponding to the classical Hamiltonian function, which represents energy, is denoted as $\hat{H}$. Once the Hamiltonian is known, the time evolution of a physical system can be determined. For a harmonic oscillator, considering only a single frequency component ω with a certain polarization, the Hamiltonian is expressed as

$$\hat{H} = \hbar\omega\left(\hat{a}^{\dagger}\hat{a} + \frac{1}{2}\right).$$

Here, $\hat{a}^{\dagger}$ and $\hat{a}$ are the creation and annihilation operators, representing the quantized (complex) amplitude of the electromagnetic field. The first term on the right-hand side, $\hat{a}^{\dagger}\hat{a}$, corresponds to the **number operator** $\hat{N} = \hat{a}^{\dagger}\hat{a}$, representing the number of photons. The second term, $1/2$, reflects the quantum fluctuations of the vacuum state where no photons are present.

Given a state with n photons, denoted as $|n\rangle$, the following relations hold

$$\begin{aligned}
&\hat{a}^{\dagger}|n\rangle = \sqrt{n+1}|n+1\rangle,\\
&\hat{a}|n\rangle = \sqrt{n}|n-1\rangle,\\
&\hat{N}|n\rangle = n|n\rangle,\\
&\hat{a}|0\rangle = 0.
\end{aligned}$$

These operators are called the annihilation and creation operators because they correspond to the annihilation and creation of photons. The linear space spanned by the set $|n\rangle(\mathrm{n} = 0,1,\ldots)$ is called the **Fock space**. The energy of a state with n photons is given by

$$\langle n|\hat{H}|n\rangle = \hbar\omega\left(n + \frac{1}{2}\right).$$

C. Coherent States of Light

In classical mechanics, the amplitude of light is proportional to the square root of its intensity (or energy). However, this relationship does not generally hold in quantum mechanics. Specifically, we cannot construct such a quantum state because we can derive $|n\rangle \neq \sqrt{n}|1\rangle$ from the expression above. Nevertheless, by superposing these discretized states, we can form a quantum state that satisfies the classical relation. This is the coherent state.

A coherent state $|\alpha\rangle$, with $\hat{a}^\dagger$ and $\hat{a}$ treated as **raising and lowering operators** respectively,[34] is expressed as[35]

$$|\alpha\rangle = \widehat{D}(\alpha)|0\rangle = \exp(\alpha\hat{a}^\dagger - \alpha^*\hat{a})\,|0\rangle = e^{-\frac{|\alpha|^2}{2}}\sum_{n=0}^{\infty}\frac{\alpha^n}{\sqrt{n!}}|n\rangle.$$

The coherent state $|\alpha\rangle$ has the following properties: (1) It is uniquely specified by the complex number α, which takes continuous values. (2) It is constructed using all basis states $\{|n\rangle|\mathrm{n} = 0,1,\cdots\}$ in the Fock space. (3) Referring to the relationship $\hat{a}|n\rangle = \sqrt{n}|n-1\rangle$, $\hat{a}|\alpha\rangle = \alpha|\alpha\rangle$ holds, making it an eigenstate of the annihilation operator with eigenvalue α. (4) Its time evolution is given by applying the unitary operator $\exp\left(-i\widehat{H}t/\hbar\right)$, leading to

$$|\alpha(t)\rangle = \exp\left(-i\widehat{H}t/\hbar\right)|\alpha\rangle = e^{-\frac{i\omega t}{2}}\left|\alpha e^{-i\omega t}\right\rangle.$$

Thus, it rotates in phase space along a circular trajectory of radius $|\alpha|$ at the frequency corresponding to the photon energy. (5) Although the proof is omitted, the coherent state achieves the minimum uncertainty product allowed by quantum mechanics. Thus, despite the inherent quantum spread due to the uncertainty principle, a large amplitude renders this spread relatively negligible, allowing the state to be represented as a point in phase space. The parameter α corresponds to the amplitude and phase of the electromagnetic field, making coherent light an electromagnetic wave with well-defined amplitude and phase.

Such electromagnetic fields can be physically realized. By repeatedly inducing the interaction $i(\alpha\hat{a}^\dagger - \alpha^*\hat{a})$ between a material possessing an electric dipole moment and propagating light, one can implement the operation corresponding to the exponential operator $\exp(\alpha\hat{a}^\dagger - \alpha^*\hat{a})$. For example, shining light into a crystal causes recursive interactions between the electric dipole moments of atoms or molecules and the light, resulting in polarization. This

[34] For the quantum harmonic oscillator, the annihilation and creation operators coincide with the ladder operators.

[35] In algebraic transformations, the bosonic commutation relation $[\hat{a},\, \hat{a}^\dagger] = 1$, the Baker-Campbell-Hausdorff formula, and the identity $\exp(-z^*\hat{a})\,|0\rangle = |0\rangle$ are used.

situation can also be realized using semiconductor junctions. The coherent light thus generated is known as solid-state or semiconductor laser light.

D. Squeezed States

A notable example of a coherent state is the **squeezed state**, which plays a central role in CV-OQC.

In general, if a state $|a\rangle$ is an eigenstate of an operator $\hat{A}$ such that $\hat{A}|a\rangle = a|a\rangle$, then for any unitary transformation $\hat{U}$, the transformed state $\hat{U}|a\rangle$ is an eigenstate of $\hat{U}\hat{A}\hat{U}^\dagger$ with the same eigenvalue a. Since $\hat{U}$ is a kind of coordinate transformation, if a coherent state can be constructed from $\hat{A}$, then a coherent state can also be constructed from the transformed operator $\hat{U}\hat{A}\hat{U}^\dagger$.

Considering $\hat{A} = \hat{a}$, the annihilation operator, the corresponding eigenstate $|\alpha\rangle = \hat{D}(\alpha)|0\rangle$ is a coherent state. Now, as a unitary transformation $\hat{U}$, define the **squeezing operator**

$$\hat{S}(z) = \hat{S}\left(re^{-i\theta}\right) = \exp\left(\frac{1}{2}\left(re^{-i\theta}\hat{a}\hat{a} - re^{i\theta}\hat{a}^\dagger\hat{a}^\dagger\right)\right)$$

with $z = re^{i\theta}$. Then the transformed operator $\hat{b}$ becomes

$$\hat{b} = \hat{S}(z)\hat{a}\hat{S}(z)^\dagger = \hat{a}\cosh r - e^{i\theta}\hat{a}^\dagger\sinh r,$$

indicating that $\hat{b}$ is a linear combination of $\hat{a}$ and $\hat{a}^\dagger$.

Next, define the **photon number operator** after transformation as $\hat{N}_{\mathrm{b}} = \hat{b}^\dagger\hat{b}$, and its eigenstates as $\hat{N}_{\mathrm{b}}|n_b\rangle = n_b|n_b\rangle$. The corresponding displacement operator is $\hat{D}_b(\beta) = \exp\left(\beta\hat{b}^\dagger - \beta^*\hat{b}\right)$. Applying $\hat{D}_b(\beta)$ to the vacuum state $|0_b\rangle$, one obtains the **squeezed state** $|\beta\rangle = \hat{D}_b(\beta)|0_b\rangle$.

Here, $\beta\hat{b}^\dagger - \beta^*\hat{b}$ is a linear combination of $\hat{b}$ and $\hat{b}^\dagger$, and $\hat{b}$ is itself a linear combination of $\hat{a}$ and $\hat{a}^\dagger$. Therefore, there exists a suitable α such that $\hat{D}(\alpha) = \hat{D}_b(\beta)$. Since $|0_b\rangle = \hat{S}(z)|0\rangle$, the squeezed state can be expressed as

$$|\beta\rangle = \hat{D}_b(\beta)|0_b\rangle = \hat{D}(\alpha)\hat{S}(z)|0\rangle.$$

In this expression, $\hat{S}(z)|0\rangle$ represents the vacuum field after squeezing, commonly referred to as the **squeezed vacuum**. Hence, the squeezed state can be regarded as the result of applying a displacement operation $\hat{D}(\alpha)$ to the squeezed vacuum.

E. Properties of Squeezed States

A squeezed state is a quantum state in which the uncertainty associated with two conjugate physical observables is redistributed: the uncertainty in one observable is reduced (squeezed) at the expense of an increased uncertainty in the conjugate one.

To describe this property, consider the operators $\hat{x} = (\hat{a} + \hat{a}^{\dagger})/2$ and $\hat{p} = -i\,(\hat{a} - \hat{a}^{\dagger})/2$, which correspond to the real and imaginary components, respectively. Let us define the operator $\hat{b}$ corresponding to the annihilation operator $\hat{a}$ transformed by the squeezing operator $\hat{S}(z)$, with $z = re^{-i\theta}$, as follows

$$\begin{aligned}\hat{b} &= \hat{S}(z)\hat{a}\hat{S}(z)^{\dagger} = (\hat{x} + i\,\hat{p})\cosh r - e^{i\theta}(\hat{x} - i\,\hat{p})\sinh r\\ &= \hat{x}\big(\cosh r - e^{i\theta}\sinh r\big) + i\hat{p}\big(\cosh r + e^{i\theta}\sinh r\big).\end{aligned}$$

In the special case where $\theta = 0$, this becomes

$$\hat{b} = \hat{x}e^{-r} + i\hat{p}\mathrm{e}^{r}.$$

This expression shows that depending on the sign and magnitude of the parameter r, either $\hat{x}$ (real part) or $\hat{p}$ (imaginary part) dominates.

For instance, the eigenstates in the limit $r = \pm\infty$ correspond to

$$\hat{x}|x\rangle = x|x\rangle,\ \hat{p}|p\rangle = p|p\rangle.$$

Although the derivation is omitted here, it can be shown that, using $|x\rangle$ as a basis, these eigenstates can be expanded as infinite sums. The coefficients (i.e., the wave functions) in these expansions take the form of delta functions or plane waves

$$|x\rangle = \frac{1}{\sqrt{\sum_x 1}}\sum_{x'}\delta(x - x')|x'\rangle,$$

$$|p\rangle = \frac{1}{\sqrt{\sum_x 1}}\sum_x e^{ipx}|x\rangle.$$

The inner product between these states is

$$\langle x|p\rangle = \frac{e^{ipx}}{\sqrt{\sum_x 1}}.$$

In the limit where quantum fluctuations are infinitely spread out, $\sum_x 1 = \infty$, leading to $\langle x|p\rangle = 0$, meaning that the states are orthogonal.

However, such infinitely extended states are not physically realizable. In practice, one considers states with finite spread, and when the spread directions are orthogonal, $\langle x|p\rangle$ asymptotically approaches 0. Such states are approximately orthogonal and can be treated as practically orthogonal in calculations.

The displacement operator $\widehat{D}(z) = \exp(\alpha\hat{a}^\dagger - \alpha^*\hat{a})$ and the squeezing operator $\hat{S}(z) = \exp\left(\frac{1}{2}(z^*\hat{a}\hat{a} - z\hat{a}^\dagger\hat{a}^\dagger)\right)$ introduced above are also used as gate operations in CV-OQC.

Appendix 2: Phase Space, the Wigner Function, and Related Topics

In Appendix 1, we introduced the coherent state and explained that it is a quantum state represented as a point in phase space (position x and momentum p), possessing properties close to those of classical states. In this appendix, we explain the **Wigner function** $W(x,p)$, which is a probability distribution (more precisely, a quasi-probability distribution) over phase space.

In classical physics, when a physical quantity $f(x,p)$ and its probability distribution $W(x,p)$ are given, the expectation value $\langle f \rangle$ is expressed as

$$\langle f \rangle = \int dpdx\, W(x,p) f(x,p).$$

To obtain the Wigner function $W(x,p)$, we trace the inverse path of the Weyl quantization, which replaces classical phase space coordinates (x,p) with quantum operators $\hat{x}$, $\hat{p}$. First, consider expressing a delta function, which takes large values when the expectation values of $\hat{x}$, $\hat{p}$ correspond to (x,p), in the form of a Fourier transform

$$\hat{\Omega}(x,p) = \underbrace{\left(\frac{1}{2\pi}\right)^2 \int d\xi d\eta\, e^{-\,i\{\xi(x-\hat{x})-\eta(p-\hat{p})\}}}_{\sim\delta(x-\hat{x})\delta(p-\hat{p})}.$$

Then, when the quantum state is $|\psi\rangle$, the Wigner function $W(x,p)$ corresponds to the expectation value of $\hat{\Omega}(x,p)$:

$$W(x,p) = \langle\psi|\hat{\Omega}(x,p)|\psi\rangle = \mathrm{Tr}\left(\hat{\rho}\hat{\Omega}(x,p)\right),$$

where $\hat{\rho} = |\psi\rangle\langle\psi|$ is the **density operator**, which can be identified with the state $|\psi\rangle$ in this case. Furthermore,

$$|\psi\rangle = \int dx'\, |x'\rangle\langle x'|\psi\rangle = \int dp'\, |p'\rangle\langle p'|\psi\rangle$$

meaning that $|\psi\rangle$ can be expressed using either the position x' or the momentum p'. By representing the wavefunction in position x as $\psi(x) = \langle x|\psi\rangle$, and noting that $e^{i(\xi\hat{x}-\eta\hat{p})} = e^{i\xi\hat{x}}e^{-i\eta\hat{p}}e^{\frac{i\hbar\xi\eta}{2}}$, we obtain the well-known form of the Wigner function

$$W(x,p) = \frac{1}{2\pi\hbar}\int d\eta\, \psi\left(x+\frac{\eta}{2}\right)\psi\left(x-\frac{\eta}{2}\right)e^{-\frac{i\eta p}{\hbar}}.$$

When using the photon number basis or the coherent state basis, one can express the operators as follows: $\hat{x} = (\hat{a} + \hat{a}^\dagger)/2, \hat{p} = -i\,(\hat{a} - \hat{a}^\dagger)/2, \alpha' =$

$i\,(\xi - i\eta)/2\,, d\xi d\eta = 4d^2\,\alpha'$, and similarly, $x = (\alpha + \alpha^*)/2\,, p = -i\,(\alpha - \alpha^*)/2$. Using the operator $D(\alpha') = \exp(\alpha'\hat{a}^\dagger - \alpha'^*\hat{a})$, we obtain

$$W(\alpha) = \left(\frac{1}{\pi}\right)^2 \int d^2\,\alpha'\, e^{-\alpha'\alpha^* + \alpha'^*\alpha} \langle\psi|D(\alpha')|\psi\rangle.$$

For example, if we set $|\psi\rangle = |0\rangle$, then since $\hat{D}(\alpha)|0\rangle = e^{-\frac{|\alpha|^2}{2}} \sum_{n=0}^{\infty} \frac{\alpha^n}{\sqrt{n!}} |n\rangle$, we obtain

$$W(\alpha) = \left(\frac{1}{\pi}\right)^2 \int d^2\,\alpha'\, e^{-\alpha'\alpha^* + \alpha'^*\alpha} e^{-\frac{|\alpha'|^2}{2}}$$

$$= \left(\frac{1}{\pi}\right)^2 \int d^2\,\alpha'\, e^{-\frac{|\alpha' + 2\alpha^*|^2}{2}} e^{-2|\alpha|^2} = \frac{2}{\pi} e^{-2|\alpha|^2} = \frac{2}{\pi} e^{-2(p^2 + x^2)}.$$

Next, let $|\psi\rangle = |\beta\rangle = D(\alpha')|0\rangle$, that is, a coherent state. Setting $\alpha' = \frac{x' + ip'}{2}$, we find

$$W(\alpha) = \frac{2}{\pi} \int d^2\,\alpha''\, e^{-\alpha''\alpha^* + \alpha''^*\alpha} \langle 0|\hat{D}(-\alpha')\hat{D}(\alpha'')\hat{D}(\alpha')|0\rangle = \frac{2}{\pi} e^{-2\left((p - p')^2 + (x - x')^2\right)}.$$

As an example, where the Wigner function cannot be regarded as a simple probability distribution, consider the so-called Schrödinger cat state. This state represents a cat in a superposition of being both alive and dead, and it is modeled here as a superposition of coherent states with opposite phases. Define

$$|\psi\rangle = \frac{1}{2}\left(\hat{D}(\alpha')|0\rangle - \hat{D}(-\alpha')|0\rangle\right)$$

and using the identity

$$\hat{D}(\pm\alpha')\hat{D}(\alpha'')\hat{D}(\pm\alpha') = \hat{D}(\alpha'' \pm 2\alpha')$$

we obtain

$$W(\alpha) = \frac{1}{2\pi}\left(e^{-2\left((p - p')^2 + (x - x')^2\right)} + e^{-2\left((p + p')^2 + (x + x')^2\right)}\right)$$

$$-\frac{1}{\pi}\cos(xp' - x'p) e^{-2(p^2 + x^2)}.$$

This expression shows that negative values appear in the vicinity of the origin. While probabilities cannot take negative values, the Wigner function can, demonstrating that the Schrödinger cat state exhibits strongly non-classical quantum behavior.

Appendix 3: Projective Measurement and Quantum Teleportation

Quantum teleportation is an operation that transfers the state of an unknown qubit at hand to a distant qubit. It is a significant application of measurement-based operations. Since it is fundamentally impossible to clone an unknown quantum state (**no-cloning theorem**), the original quantum state is destroyed in the process of transfer. For this reason, the operation is referred to as teleportation rather than duplication. Quantum teleportation plays an essential role in implementing operations equivalent to cubic phase gates, as well as in the swapping of quantum states in MBQC.

Quantum teleportation consists of two steps: a **projective measurement** known as **Bell measurement** and a classical communication process (**feed-forward**).

For simplicity, the following explanation uses qubits (see Figure A1). A projective measurement involves measurement with operators $\hat{P}_n$ that satisfy $\{\hat{P}_n \mid \sum_n \hat{P}_n = \hat{I}, \hat{P}_n\hat{P}_n = \hat{P}_n\}$. Each operator $\hat{P}_n$ is called a **projection operator**. In particular, measurement based on projection onto a basis known as the Bell basis is called a Bell measurement. The Bell basis for two qubits consists of the following four entangled states $|\mathrm{Bell}\ 1\rangle$ to $|\mathrm{Bell}\ 4\rangle$, and the measurement that projects onto these states constitutes a Bell measurement. The projection operator $\hat{P}_n$ $(n = 1,2,3,4)$ is given by

$$\hat{P}_n = |\mathrm{Bell}\ n\rangle\langle\mathrm{Bell}\ n|.$$

Through Bell measurement, one can determine which of the four Bell states the system is in.

The actual operation proceeds as follows. The operator $\hat{H}$, known as the Hadamard gate, performs a rotation of the qubit state around the x-axis by 45 degrees, effectively mixing the basis states $|0\rangle$ and $|1\rangle$. It is represented by the matrix

$$\hat{H} = \frac{1}{\sqrt{2}}\begin{pmatrix} 1 & -1 \\ 1 & 1 \end{pmatrix}.$$

Quantum teleportation is carried out in two stages (see Figure A2). In the first stage, an entangled state is generated between the auxiliary port b and the destination c. In the second stage, a Bell measurement is performed on part of that entangled pair together with the input qubit a, which is in the unknown state $\alpha|0\rangle_a + \beta|1\rangle_a$. The result of the measurement is then used to modify the output accordingly, resulting in the state $\alpha|0\rangle_c + \beta|1\rangle_c$, which completes the teleportation.

These operations can be directly extended to the CV quantum case, owing to the correspondence between DV gate operations and CV ones described earlier. Even the Hadamard gate, which was not previously addressed, can be implemented in the CV setting using a single half-mirror (or in the case of optical waveguide circuits, a directional coupler) to realize the circuit that generates Bell states through a combination of a Hadamard gate and a CNOT gate.

Figure A1 Projection onto Bell States and Bell Measurement

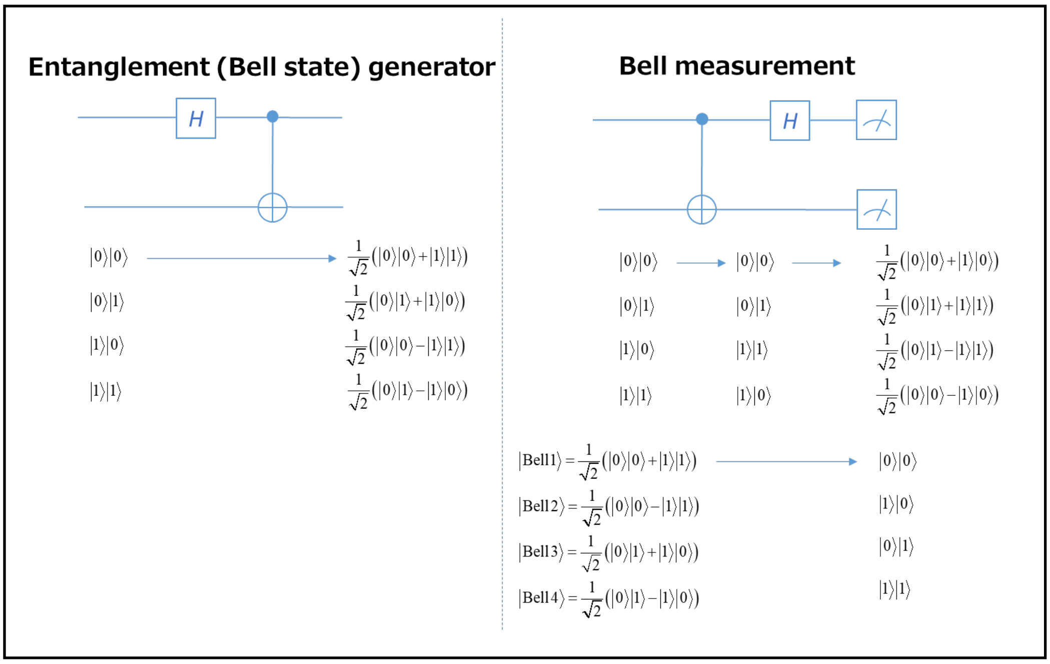

Figure A2 Quantum Circuit for Quantum Teleportation

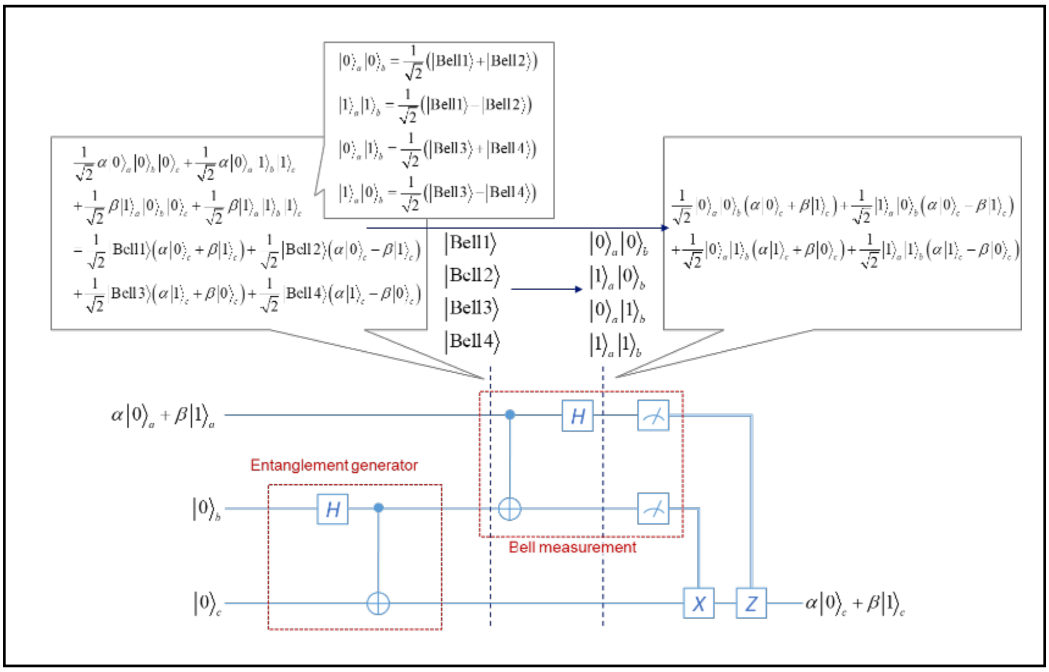

Appendix 4: Generation of Entangled Squeezed States via Beam Splitter

A beam splitter is a device that divides incident light into two or more separate directions. In quantum optics, a half-mirror serves this purpose. The quantum mechanical description of optical beam splitting is as follows.

Let us denote one output region as A and the other as B. At their interface, we consider the annihilation operator $\hat{a}_B$ that removes a photon from region B and the creation operator $\hat{a}_A^\dagger$ that generates a photon in region A, and vice versa, $\hat{a}_A$ for annihilation in A and $\hat{a}_B^\dagger$ for creation in B. The operation of passing through the beam splitter corresponds to applying the operator

$$\hat{S} = e^{i\pi/2}(\hat{a}_A^\dagger \hat{a}_B - \hat{a}_A \hat{a}_B^\dagger)$$

with a certain probability.

Here, the negative sign arises from boundary conditions, and it may apply to either the transition from A to B or from B to A. The phase factor $e^{i\pi/2}$ is the phase shift associated with a transition between regions. While such phase shifts can be derived from solving classical electromagnetic boundary problems, in the quantum framework, they arise from the requirement that $\hat{S}$ be Hermitian so that the total probability is conserved (i.e., sums to one).

In waveguide devices, optical pulses propagate while the operator $\hat{S}$ acts continuously. By adjusting the propagation length, one can achieve a beam splitter with 50% reflectance and transmittance. In the case of a thin-film mirror, this 50% splitting can be achieved by tuning the reflectance. The corresponding operator is defined as

$$\hat{B}_{\mathrm{half}} \stackrel{\mathrm{def}}{=} \exp\left(-\frac{\pi}{4}\left(\hat{a}_A^\dagger \hat{a}_B - \hat{a}_A \hat{a}_B^\dagger\right)\right).$$

Now, consider injecting into ports A and B two vacuum-squeezed states with equal squeezing level r but orthogonal squeezing directions, namely $\hat{S}(-r)|0\rangle_A$ and $\hat{S}(r)|0\rangle_B$. Then, after passing through the beam splitter, the resulting state becomes

$$\hat{B}_{\mathrm{half}}\ \hat{S}(-r)|0\rangle_A \otimes \hat{S}(r)|0\rangle_B = \exp\left(r\left(\hat{a}_A^\dagger \hat{a}_B^\dagger - \hat{a}_A \hat{a}_B\right)\right)|0\rangle_A \otimes |0\rangle_B$$

$$= \sqrt{1-q^2}\sum_{n=0}^{\infty} q^n |n\rangle_A \otimes |n\rangle_B$$

where $q = \tanh r$. This clearly shows that the resulting state exhibits quantum entanglement with correlated photon number n. This type of entangled state is known as the **EPR** (**Einstein–Podolsky–Rosen**) state.

The intuition behind the generation of such entanglement is illustrated in Figure A3. Although a squeezed wave cannot be represented as a classical wave due to its intrinsic quantum uncertainty i.e., fixing the phase or amplitude leads to uncertainty in the conjugate variable. The diagram schematically depicts the squeezed wave as composed of even-photon-number components represented by two coherent waveforms.

By injecting squeezed light and its phase-shifted counterpart from opposite sides of a beam splitter, the resulting interference produces an entangled state. This state, originally proposed by Einstein, Podolsky, and Rosen as a paradox, corresponds to a quantum state in which joint measurements of position and momentum (or conjugate variables) for the whole system become possible. As such, it represents a strongly entangled quantum state and serves as a vital computational resource in quantum information processing.

Figure A3 Illustration of Entangled Squeezed Light via Beam Splitter